

DEVELOPMENT AND CHARACTERIZATION OF A NEW VERY HIGH-
PRESSURE STRAND BURNER FOR STUDYING PROPELLANT BURNING
RATES AT EXTREME TEMPERATURES

A Thesis

by

CATHERINE ANNE MARIE DILLIER

Submitted to the Office of Graduate and Professional Studies of
Texas A&M University
in partial fulfillment of the requirements for the degree of

MASTER OF SCIENCE

Chair of Committee,	Eric L. Petersen
Committee Members,	Waruna Kulatilaka
	Chad Mashuga
Head of Department,	Andreas A. Polycarpou

December 2016

Major Subject: Mechanical Engineering

Copyright 2016 Catherine Anne Marie Dillier

ABSTRACT

For years, additives have been used to tailor solid propellant behavior for specific applications. The propellant is often exposed to harsh environments during combustion such as extreme temperatures and high pressures. While the burning rates of AP/HTPB-based solid rocket propellants up to pressures of 2000 psi are well documented, relatively little data at higher pressures exists. Therefore, a new high-pressure, constant-volume strand burner facility has been installed and characterized at Texas A&M University to test pressures up to 10,000 psi. The design is primarily based on the current test vessel, strand burner II or SB-II and includes a cylindrical main body, two endcaps, and a bolt which is used to hold the test specimen. In addition to high-pressure testing, the new strand burner will be used to determine the temperature sensitivity of AP/HTPB-based solid propellants at high and low temperatures. For low-temperature tests, the strand burner will be placed horizontally into a freezer and cooled to -65°F; whereas for the high-temperature tests, the strand burner will be heated to 194°F using resistance heating tape and mounted vertically.

Two 80% monomodal AP/HTPB composite baseline propellant formulations were used to verify the new strand burner's design, one with an average AP particle size of 200 μm and the other, 138 μm . The resulting burning rates and temperature sensitivities were compared to historical data with good agreement, thus validating the new strand burner facility and experimental procedures. This thesis details the development and characterization of the new high-pressure strand burner.

ACKNOWLEDGMENTS

I would like to thank my advisor and committee chair, Dr. Petersen, for his never-ceasing guidance, support, and patience as I completed this project and throughout my time in his lab. It has provided countless rewarding opportunities to grow as a researcher, and more importantly, a person, and I cannot thank him enough. His dedication to his research and students is something I strive to emulate. I would also like to thank my other committee members, Drs. Kulatilaka and Mashuga for serving on my thesis committee.

Additionally, I would like to thank my fellow researchers and friends at the Texas A&M Turbomachinery Laboratory: Chris Thomas, Gordon Morrow, and particularly Andrew Demko, Jacob Stahl, and Thomas Sammet for volunteering their time and effort. Whether it was installing plumbing and wiring or running to Home Depot to purchase supplies or simply loading the strand burner components in and out of my car, these three men helped tremendously and I greatly appreciate their assistance. I would also like to thank my other co-workers who helped troubleshoot problems as they arose. I appreciate your time, effort, and most importantly, advice.

Finally, thank you to my family, particularly my parents James and Doreen, for their continuous encouragement and loving support. I would not be where I am without them. I would also like to thank my friends for listening to my non-stop ‘shop’ talk during this project. I greatly appreciate their patience and support. I would not have made it this far without it.

CONTRIBUTORS AND FUNDING SOURCES

Contributors

This work was supervised by a thesis committee consisting of Professors Eric L. Petersen and Waruna Kulatilaka of the Department of Mechanical Engineering and Professor Chad Mashuga of the Department of Chemical Engineering.

All work for the thesis was completed by the student, under the advisement of Dr. Eric L. Petersen of the Department of Mechanical Engineering.

Funding Sources

This work was made possible in part by Helicon Chemical Company, LLC under a Phase 2 SBIR from the U.S. Navy, Agreement Number N68335-16-C-0032.

Its contents are solely the responsibility of the author and do not necessarily represent the official views of Helicon Chemical Company, LLC.

NOMENCLATURE

HTPB	Hydroxyl-Terminated Polybutadiene
AP	Ammonium Perchlorate
IPDI	Isophorone Diisocyanate
ASME BPVC	ASME Boiler and Pressure Vessel Code
SB-II	Strand Burner II (current vessel)
SB-IV	Strand Burner IV (new vessel)
DAS	Data Acquisition System

TABLE OF CONTENTS

	Page
ABSTRACT	ii
ACKNOWLEDGMENTS	iii
CONTRIBUTORS AND FUNDING SOURCES	iv
NOMENCLATURE	v
TABLE OF CONTENTS	vi
LIST OF FIGURES	viii
LIST OF TABLES	xi
1. INTRODUCTION	1
1.1 Solid Propellant Fundamentals	1
1.2 Burning Rates	2
1.3 Temperature Sensitivity	3
1.4 Objective	4
2. LITERATURE REVIEW	5
2.1 Strand Burners	5
2.2 Temperature Sensitivity	7
3. EXPERIMENTAL DESIGN	12
3.1 Strand Burner Design	12
3.1.1 Main Body and End-Caps	12
3.1.2 Sample Holder	19
3.1.3 Engineering Analysis	21
3.2 Facility Hardware	24
3.3 Testing Procedures	34
3.3.1 Burning Rates	34
3.3.2 Temperature Sensitivity	36
3.4 Characterization	40
3.4.1 Pressure Transducer Calibration	40
3.4.2 Comparison to SB-II	43
3.4.3 High-Pressure Results	47

3.4.4 Temperature Sensitivity Results	50
3.4.5 Uncertainty	53
4. CONCLUSION	56
4.1 Summary	56
4.2 Challenges	57
4.3 Recommendations	59
REFERENCES	61
APPENDIX A: MECHANICAL PROPERTIES OF 17-4 PH STAINLESS STEEL	64
APPENDIX B: STRAND BURNER IV DRAWINGS	65
APPENDIX C: FACILITY HARDWARE	74

LIST OF FIGURES

	Page
Figure 1. Burning rate results for 80% monomodal AP/HTPB composite propellants at -18.4° and 167°F ²¹	8
Figure 2. Temperature sensitivity for 85% bimodal AP/HTPB composite propellants at -18.4° and 167°F ²¹	9
Figure 3. Compilation of temperature sensitivities of ammonium perchlorate at varying initial temperatures and AP particle sizes copied directly from Boggs et. al. ²²⁻²⁷	10
Figure 4. Expanded view of SB-IV.	16
Figure 5. Crane used to lift and move SB-IV.	17
Figure 6. Internal view of the nickel plating on the end-cap face with the sample holder screwed in.	18
Figure 7. Original sample holder with the head sheared off and the remaining portion still in the end-cap.	20
Figure 8. Second sample holder.	21
Figure 9. Vertically assembled SB-II.	24
Figure 10. Vertically assembled SB-IV.	24
Figure 11. Nitrogen bottles used to fill and purge vessel before and after tests.	25
Figure 12. New (right) and existing (left) control panels for remote operation during experiments.	26
Figure 13. Mini-Hippo air piston used as the fill pneumatic valve.	27
Figure 14. Hipco diaphragm air operator used as the exhaust pneumatic valve.	27
Figure 15. Gas booster used to compress the incoming Nitrogen to pressures above 6,000 psi.	28
Figure 16. Air compressor used to supply air to the gas booster.	29
Figure 17. Plumbing schematic of experimental setup.	30

Figure 18. New experimental setup for high pressure and temperature sensitivity experiments.....	31
Figure 19. Pressure transducers and quarter turn valve connecting to the vertical setup used for high pressure and high-temperature tests.	32
Figure 20. FLUKE thermometer used to monitor and record the temperature detected by the thermocouple located inside the vessel.....	33
Figure 21. Thermocouple port with cap in place of thermocouple for high-pressure testing.....	34
Figure 22. Sample pressure and light-emission data plot taken from experiments using SB-II.	35
Figure 23. Example loading of propellant sample in the modified bolt using Nichrome wire ignition.....	36
Figure 24. SB-IV placed into the freezer for low-temperature sensitivity tests.....	37
Figure 25. Freezer control panel used to set the freezer temperature.....	38
Figure 26. Heating tape wrapped around SB-IV for high-temperature sensitivity tests. The same vertical mount is used for high-pressure testing.....	39
Figure 27. Pressure calibration for the new GageScope pressure transducer using the existing system.....	42
Figure 28. Calibration for the pressure transducer used to measure 'real time' vessel pressure using the existing system.....	43
Figure 29. Burning rate data collected using both SB-II and SB-IV for an 80% monomodal propellant batch with an average AP particle size of 200 μ m.	45
Figure 30. Example pressure trace collected using SB-II for an 80% monomodal propellant, average AP particle size of 200 μ m, at an average test pressure of 1767 psi.	46
Figure 31. Example pressure trace collected using SB-IV during preliminary pressure testing for an 80% monomodal propellant, average AP particle size of 200 μ m, at an average test pressure of 1739 psi.	47
Figure 32. Example pressure trace collected using SB-IV for an 80% monomodal propellant, average AP particle size of 138 μ m, at an average test pressure of 8193 psi.....	49

Figure 33. High pressure burning rate data collected using the new SB-IV for an 80% monomodal propellant with an average AP size of 138 μm (Base 03).	50
Figure 34. Example temperature sensitivity data collected using the new high pressure strand burner for an 80% monomodal propellant with an average AP particle size of 138 μm	52
Figure 35. Example uncertainty in time measurement using SB-IV.....	55

LIST OF TABLES

	Page
Table 1. Overview of current strand burners and their maximum test pressures ^{6-8,16-20}	7
Table 2. Calculated minimum ASME BPVC design parameters compared to the actual.	15
Table 3. Calculated stress values and corresponding locations.	22
Table 4. Comparison of SB-IV to SB-II.	23
Table 5. Propellant formulations used in characterization tests for the new high-pressure strand burner.	44
Table 6. Comparative temperature sensitivity data for 80% monomodal propellants using SB-II and SB-IV.	52

1. INTRODUCTION

1.1 Solid Propellant Fundamentals

Solid propellants are either a homogeneous or a heterogeneous mixture of oxidizer and fuel, which can self-sustain combustion upon ignition. They are used in a variety of applications such as space flight and airbags due to their many advantages, including simplicity, repeatability, and a wide range of burning rates¹. Solid propellants are typically cast into motors which are then placed in combustion chambers. The chemical energy produced during combustion is converted into thermal energy and ultimately kinetic energy through an exit nozzle. The amount of energy produced varies due to a variety of factors including classification.

There are two main solid propellant classifications: double-base and composite¹. Double-base propellants are a homogeneous mixture of fuel and oxidizer, usually nitrocellulose and nitroglycerin. In contrast, composite propellants are a heterogeneous mixture consisting of three main ingredients: hydrocarbon binder, which can also act as a fuel source, crystalline oxidizer, and curing agent. Additionally, solid propellants are typically either monomodal, bimodal, or trimodal with respect to crystalline oxidizer particle size. Monomodal propellants have only one average oxidizer particle size, while bimodal and trimodal propellants have two and three, respectively. Solid propellants can also vary based on the percent-by-mass of oxidizer in the propellant. The Petersen Group at Texas A&M University typically studies either 80% monomodal or 85% bimodal propellants; where the 80% monomodal propellants are 80%-by mass AP with one AP

particle size, and the 85% bimodal are 85%-by mass AP with two AP sizes, fine and coarse. The propellants used in this study were 80% monomodal, AP/HTPB composite propellants, using hydroxyl-terminated polybutadiene (HTPB) as the binder, ammonium perchlorate (AP), the crystalline oxidizer, and isophorone diisocyanate (IPDI), the curing agent.

In addition to these primary ingredients, additives can be included to help tailor solid propellant properties, such as strength or burning rate, for specific applications¹⁻². Bonding agents help increase the strength by further cross-linking the binder and crystalline oxidizer, while plasticizers help lower the propellant viscosity during mixing. Similarly, metal catalysts such as iron oxide or lead stearate help increase the burning rate. In recent years, the Petersen Research Group at Texas A&M University has been extensively researching the use of titanium dioxide (TiO₂) and nanoscale aluminum as catalysts to improve the burning rate of AP/HTPB-composite propellants³⁻⁴.

1.2 Burning Rates

As previously mentioned, solid propellants are used in a variety of applications where the burning conditions dictate the type of propellant used. Depending on the environment, solid propellants will behave differently, particularly their burning rates. While a multitude of factors affect the burning rate, pressure is typically the most important. For example, the chamber pressure of a motor varies depending on mission, desired thrust level, design, etc.; hence knowing how a propellant's burning rate changes with pressure is extremely important. The relationship between pressure and burning rate

is empirically expressed as the power law shown in Equation 1 known as either St. Robert's Law or Vieille's Law^{1,5}.

$$r = aP^n \quad (1)$$

In the above equation, r represents the burning rate, a , the temperature coefficient, P , the initial chamber pressure, and n , the burning rate exponent; n is also known as the combustion index and describes the effect of chamber pressure on the burning rate. The values for a and n are experimentally determined based on the propellant's composition. When plotted on a log-log scale, this correlation appears linear.

1.3 Temperature Sensitivity

In addition to pressure, the combustion chamber temperature greatly affects solid propellant burning rates. Since solid propellants are used in a variety of applications, they are often exposed and expected to perform in harsh environments such as extreme hot and cold temperatures. Air-launched missile motor temperatures, for example, can range from -65°F to 160°F¹. The effect of temperature on the burning rate is referred to as temperature sensitivity, which is the percent change of burning rate per degree change in propellant temperature at a particular chamber pressure¹. This relationship is shown as Equation 2,

$$\sigma_P = \left(\frac{d \ln r}{dT} \right)_P \quad (2)$$

where r is the average burning rate and T , the initial temperature^{1,5}. Temperature sensitivity is usually determined from experimental data.

1.4 Objective

While there are many existing facilities to study burning rates and temperature sensitivity, there are few that fulfill both requirements. The current strand burner at Texas A&M University is only designed for determining propellant burning rates up to 5,000 psi and does not incorporate a way to consistently measure temperature sensitivity. Therefore, the objective of this study was the development and characterization of a new strand burner facility for determining both burning rates at very high-pressures and temperature sensitivities for propellants. Chapter 2 provides a literature review of current strand burners and propellant temperature sensitivities. An extensive description of the new facility and strand burner is presented in Chapter 3 along with the associated new testing procedures and results used to verify the design capabilities. This thesis concludes with an overview of the challenges associated with this project and recommendations for further improvements.

2. LITERATURE REVIEW

2.1 Strand Burners

There are three primary methods for collecting burning rate data: small-scale ballistic evaluation motors, full-scale motors, and strand burners, often called Crawford burners or bombs¹. Small-scale motors are useful for preliminary tests but usually produce slightly lower burning rates than full-scale motors due to scaling factors. While full-scale motors produce the most real-application burning behaviors, they are often expensive and time-consuming, making them less desirable for testing new propellant formulations. Strand burners, however, are ideal for characterizing the behaviors of new propellant formulations. They are small, constant-volume pressure vessels in which propellant strands can be burned under a variety of initial pressures and temperatures to simulate combustion chamber conditions.

The first strand burner was introduced by Crawford in 1947⁶. It consisted of a stainless steel cylindrical body, lid, and cap and used nichrome wire ignition. The original design also included a large, glass window for burning rate measurements using photography at pressures up to 2000 psi. The window was later removed to safely test at higher pressure up to 5000 psi, where fuse wires were used instead of photos to determine burning rates. Since Crawford's original strand burner, various burning rate measurement techniques and strand burners have been developed across the country.

As previously mentioned, a variety of techniques can be used to determine solid propellant burning rates. The most common technique is using a high-speed camera to

record the burn and using the resulting video to determine the beginning and end burn times⁶⁻¹⁰. Other techniques include X-ray, microwave interferometry, optical, laser fractional light transmission, and phototransistor methods¹¹⁻¹⁵. For this study, the pressure method, which uses the inflection points from the pressure trace recorded during the burn, to determine start and end burn times. Further details about this method are described in subsequent sections.

Although there are multiple burning rate measurement techniques, most current strand burners are based on the original Crawford bomb described in Crawford, et. al.⁶. Strand burners typically consist of constant-volume pressure vessels with optical ports for varying diagnostics. Table 1 gives an overview of several current strand burners and their maximum working pressures. Although the working pressures may be higher, most of the researchers listed only test pressures up to about 1,100 psi, with the exception of Crawford and Petersen and coworkers. Crawford typically tested pressures up to 5,000 psi, while the Petersen Research Group at Texas A&M University usually tests between 500 and 2,000 psi^{6,16}. As a result, while the burning rates of AP/HTPB-based composite solid propellants up to pressures of 2,000 psi are well documented, relatively few data at higher pressures exist. Therefore, the focus of this study was the development and characterization of a new very high-pressure, constant-volume strand burner facility at Texas A&M University to test pressures up to 10,000 psi. This new strand burner doubles the current pressure testing capabilities of the Petersen Research Group and can also be used for determining the temperature sensitivity of propellants.

Table 1. Overview of current strand burners and their maximum test pressures^{6-8,16-20}.

Primary Investigator, Location	Maximum Test Pressure (psi)
B. L. Crawford, University of Minnesota, Minneapolis, MN	5,000
E. L. Petersen, Texas A&M University, College Station, TX	10,000 (this work)
S. Son, Purdue University, Wes Lafayette, IN	6,000
T. L. Boggs, Naval Weapons Center, China Lake, CA	6,000
E. W. Price, Georgia Institute of Technology, Atlanta, GA	2,000
M. Q. Brewster, University of Illinois at Urbana-Champaign, Urbana, IL	1,000
S. R. Chakravarthy, Indian Institute of Technology, Madras, India	2,000
S. T. Thynell, The Pennsylvania State University, University Park, PA	1,000

2.2 Temperature Sensitivity

As described before, temperature sensitivity is the effect of initial temperature on the burning rate. Solid propellants are used in a variety of environments and can be exposed to harsh combustion conditions such as extreme, high and low temperatures. Determining the effects of temperature on the burning rate therefore becomes vastly important during the design process. Past studies, particularly Demko, et. al., have shown burning rate increases and decreases for higher and lower initial propellant temperatures, respectively, as shown in Figure 1²¹. The propellants used in the aforementioned study were 80% monomodal AP/HTPB composite propellants tested at -

18.4 and 167°F. Demko et. al. also showed that the calculated propellant temperature sensitivity for an 85% bimodal AP/HTPB composite propellant decreased with pressure at the lower and higher temperatures, ultimately converging at a pressure of 2000 psi²¹. These results are shown in Figure 2. Boggs and several other studies, compiled in Figure 3, showed similar results for a single AP crystal at higher temperatures²²⁻²⁷. Figure 3 also illustrates the inconsistencies in temperature sensitivity for AP crystals due to various initial temperatures and particle sizes.

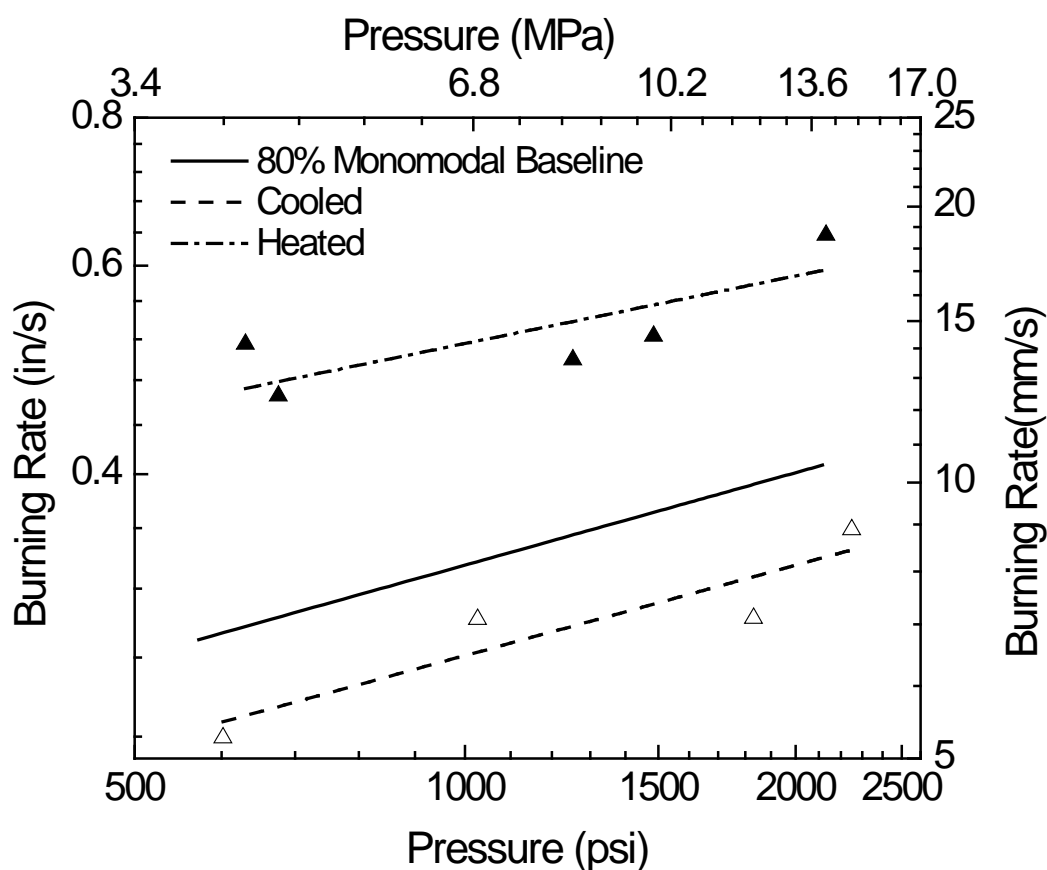


Figure 1. Burning rate results for 80% monomodal AP/HTPB composite propellants at -18.4° and 167°F²¹.

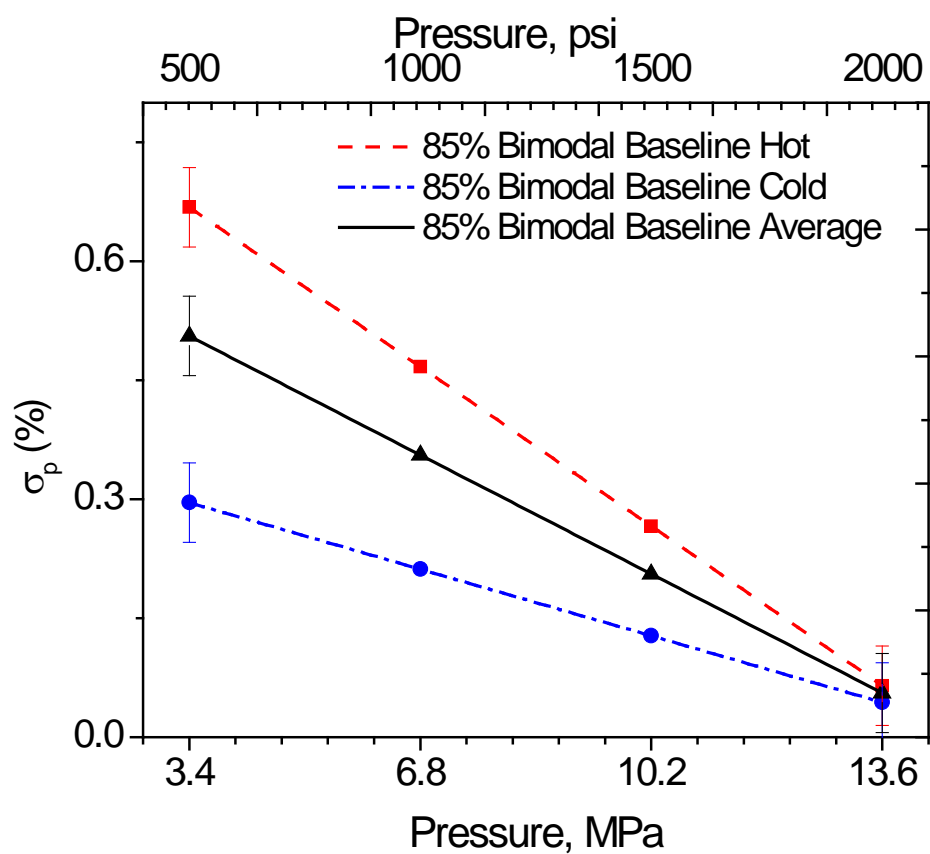


Figure 2. Temperature sensitivity for 85% bimodal AP/HTPB composite propellants at -18.4° and 167°F^{21} .

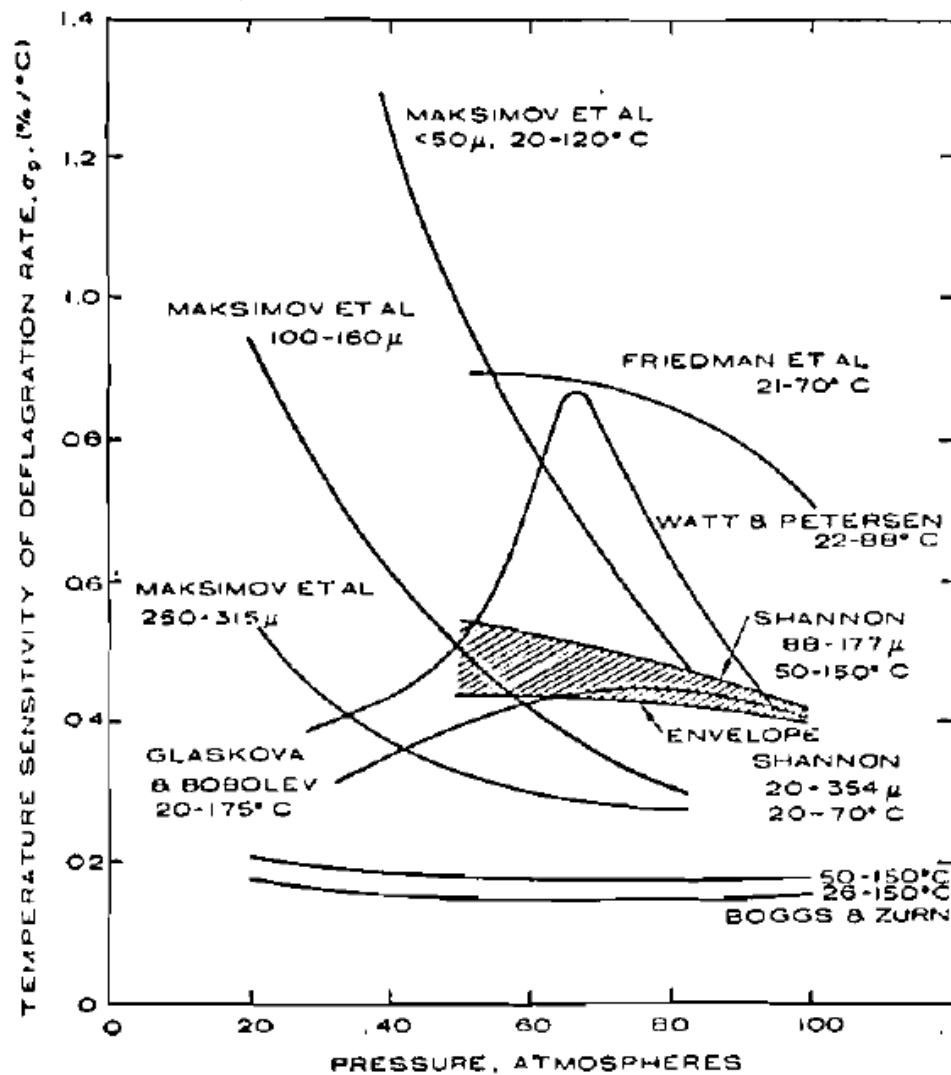


Figure 3. Compilation of temperature sensitivities of ammonium perchlorate at varying initial temperatures and AP particle sizes copied directly from Boggs et. al.²²⁻²⁷.

Since numerous variables can affect a propellant's temperature sensitivity, the method for evaluating temperature sensitivity becomes extremely important. Over the past years, multiple techniques have been developed for testing propellants at elevated temperatures. One procedure, performed by Shannon et al., entailed leaving the

propellant samples in an oven for a minimum of 18 hours, then burning them within seven minutes of removal²⁶. Other methods included using a “thermal block” where the samples sat on a block heated by hot fluid²⁵. The method used in the present study was developed by Boggs et al. and involves wrapping heating tape around the strand burner main body²². A detailed description of the high-temperature sensitivity measurements follows in a later section.

While there are a variety of methods for the high-temperature tests, there are very few for the low-temperature tests. The previous method used by the Petersen Research Group at Texas A&M University included lowering the propellant temperature in 3 stages so as to prevent rapid cooling and damage to the propellant. For the first stage, each sample was placed into an ethylene glycol and ethanol bath to cool the samples to -50°C. Afterwards, the samples were placed in dry ice to lower their temperature to -78.5°C; then another bath of liquid N₂ and ethanol to reach a final temperature of -120°C. The propellants were then tested within 3 minutes of removal so as to ensure a relative initial temperature of -28°C. Further details for this process can be found in Demko et. al²¹. While this process is economical and simple to implement, there are several possible sources of error, particularly at the higher pressures. As the combustion chamber is pressurized, the room-temperature inert gas warms the propellant, causing the propellant’s initial temperature to vary. Therefore, a new method for measuring low-temperature sensitivity was developed and implemented as part of this study.

3. EXPERIMENTAL DESIGN

3.1 Strand Burner Design

3.1.1 Main Body and End-Caps

The new strand burner design was primarily based on the existing test vessel, strand burner II or SB-II, which is thoroughly described by Carro et al.¹⁶. It includes a main body, two end-caps, and a bolt which is used as the propellant sample holder.

While SB-II can test pressures up to 5,000 psi, the new high-pressure strand burner, strand burner IV or SB-IV, doubles this with the ability to test up to 10,000 psi.

Additionally, SB-IV will be used to determine temperature sensitivity of composite solid propellants. Since SB-IV will be exposed to significantly higher pressures, safety was the paramount design aspect. As a result, unlike SB-II, which has four windows for various diagnostic techniques, SB-IV has none.

To ensure the safety and operational success of SB-IV, engineering formulas were used to ensure quantitatively that the mechanical components would not fail. These calculations were made utilizing thick-walled pressure vessel design formulas available in Section VIII Division I of the ASME Boiler and Pressure Vessel Code (ASME BPVC)²⁸. These formulas are industry standard in pressure vessel design and its components, having been approved by a committee of experienced engineers. To further increase safety, a design pressure of 15,000 psi was used when calculating the dimensions of SB-IV, which is 50% greater than the normal operating pressure of 10,000 psi. Additionally, a safety factor of four along with the yield strength, which is less than

the ultimate tensile strength, was used to calculate the maximum allowable stress.

Equation 3 shows the relationship between maximum allowable stress, yield strength, and safety factor,

$$\sigma_{allowable} = \frac{\sigma_{yield}}{SF} \quad (3)$$

where $\sigma_{allowable}$ is the maximum allowable stress, $\sigma_{ultimate}$ is the yield strength, and SF is the safety factor.

One primary difference between SB-IV and SB-II is the material. SB-II uses a low-carbon steel alloy (SAE 4140), while SB-IV consists of stainless steel 17-4PH. The material was primarily changed due to design constraints. Since SB-IV will also be used for low-temperature sensitivity tests, the entire test vessel must fit within a particular freezer; hence, the final dimensions are constrained by the freezer's. Therefore, given the higher pressures and dimensional restraints, the material was changed to 17-4PH due to its significantly higher yield and tensile strengths. SAE 4140 has a yield strength of only 60.2 ksi, whereas 17-4 PH has an average yield strength of almost double at 110 ksi. Although the material changed, the overall internal volume of SB-IV remained the same as SB-II. The full mechanical properties of 17-4 PH can be found in Appendix A.

The same internal diameter of 3.70 in and internal height of 6 in, volume of 76.76 in³, were used to ensure the same pressure rise during burning in SB-IV as in SB-II. As the propellant burns in the constant-volume vessel, the temperature and subsequently, the pressure, both rise. This pressure increase varies depending on the propellant formulation but typically lies within 15 to 20% of the initial pressure for low-pressure testing (~600 psi) and 5 to 8% for high-pressure testing (≥ 2000 psi)¹⁶. Ideally,

the samples should be burned in a constant-pressure environment, but previous studies have proven this slight pressure increase to be inconsequential²⁹. Additionally, when calculating the propellant burning rate, the average test pressure is used.

The final design dimensions were calculated using the following equations from the ASME BPVC,

$$t_{shell} = R_{inside} * \left(Z^{\frac{1}{2}} - E \right) \quad (4)$$

$$t_{endcap} = 2 * R_{inside} \sqrt{\frac{C * P_{design}}{\sigma_{allowable} * E}} \quad (5)$$

where t_{shell} is the shell thickness, R_{inside} , the internal radius, Z , a dimensionless parameter given in Equation 6, E is 1 for a seamless shell, $t_{end-cap}$, the end-cap thickness; C is 0.3 for threaded enclosures, and P_{design} , the design pressure²⁸.

$$Z = \frac{\sigma_{allowable}^{E+P_{design}}}{\sigma_{allowable}^{E-P_{design}}} \quad (6)$$

The maximum allowable stress was calculated as 27.5 ksi using Equation 3. The final outer diameter and end-cap thickness were slightly increased as additional safety factors and for material purchasing reasons. Additionally, according to the ASME BPVC, it states that for a threaded end-cap, the minimum number of threads engaged needs to be at least ten for the target design diameter size²⁸. For this reason, the end-cap incorporated three inches of 4.0-4 UNC sized threads to ensure compliance. Table 2 compares the calculated ASME BPVC minimum acceptable and actual dimensions.

Table 2. Calculated minimum ASME BPVC design parameters compared to the actual.

Parameter	Units	ASME BPVC Min.	Actual	% Increase
R_{outer}	in	-	3.75	-
R_{inside}	in	-	1.85	-
t_{shell}	in	1.56	1.90	21.8
$t_{end-cap}$	in	1.50	1.75	16.7
End-Cap Threads	-	10	12	20

The body and end-caps were machined out of solid rods of 17-4 PH stainless steel. The 12 in main body has an outer diameter of 7.5 in and an inner diameter of 3.7 in. Each end has 3-in-deep, 4.0-4 UNC internal threads to accept the end-caps. The threads are coated with copper anti-seize to prevent seizing and are screwed into the main body using a custom key. Both end-caps have the same overall dimensions. The 8.5 in hexagonal head of each end-cap is 1.75 in thick, making the overall length of the strand burner 15.5 in. On the internal face of the hexagonal head of each end-cap is a 0.31-in-wide by 0.20-in-deep groove for a face-sealing O-ring. Additionally, past the threads on each end-cap is an O-ring groove 0.24 in wide by 0.12 in deep. These two O-rings are coated in vacuum grease and used to seal the strand burner forward and aft. High-strength polyurethane O-rings were chosen due to their resistance to wear and tearing and their temperature range of -40°F to 200°F.

While the overall dimensions are the same for both end-caps, each end has different ports. The original bottom end-cap had a center 1”-8 UNF tapped hole to receive the sample holder. Unfortunately, during initial pressure testing, the sample

holder seized in the end-cap and ultimately had to be drilled out. As a result, the center tapped hole was modified to a 1-1/16"-12 UNF tapped hole. All other dimensions remained the same. The other end-cap, used for filling and venting, has two ports. The first port is used for both filling and venting the pressure vessel and consists of a 9/16"-18 UNF thread leading to a 0.22 in deep hole which then reduces to a 0.09 in hole. Next to it is a 0.22 in hole leading to another 9/16"-18 UNF thread. This second port is used to insert a thermocouple from Conax during temperature sensitivity tests. Figure 4 shows an expanded view of SB-IV's main components: the main body, two end-caps, and a modified bolt which serves as the sample holder. Detailed drawings of SB-IV are located in Appendix B.

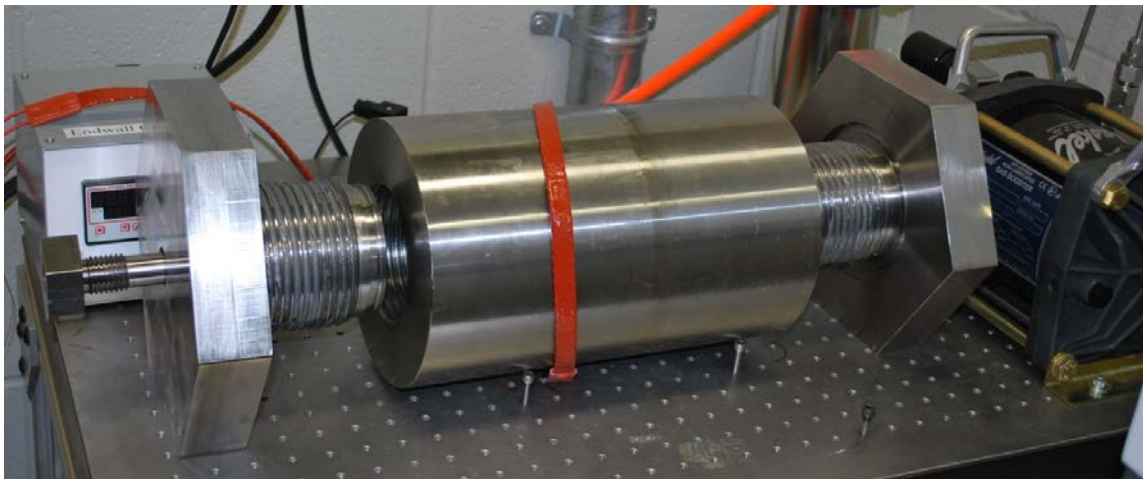


Figure 4. Expanded view of SB-IV.

Since SB-IV will be used for both low- and high-temperature sensitivity tests, it must be easily transportable between a vertical stand and the freezer used for the low-temperature tests. Thus, to easily remove the sample holder between tests and alternate

between the vertical stand and freezer, SB-IV is held by four, 1.50 in thick aluminum braces with 1.5 in wide L-brackets attaching them to the vertical stand. SB-IV can be removed from the vertical stand without difficulty by simply removing the bolts mounting the L-brackets to the vertical stand. However, since the entire assembled strand burner weighs approximately 220 lbs, a crane must be used to lift and place SB-IV into the freezer. Figure 5 shows the crane with straps attached to SBIV.



Figure 5. Crane used to lift and move SB-IV.

The entire internal surface of the main body, not including the threads, and both end-cap faces are coated with a 0.003 in thick nickel plating to prevent corrosion from combustion product residues. While 17-4 PH is resistant to most corrosives, it is not resistant to salts. The Petersen Research Group at Texas A&M University typically uses

ammonium perchlorate, a salt, as the propellant oxidizer, so salt-corrosion resistance was a design concern. The nickel coating is highly resistant to salts and other products and is often used in sub-sea applications. The nickel plating, or nickel electro-deposition, is applied using an electrical current. In addition to providing corrosion-resistance, the nickel plating also improves the hardness and resistance to wear of the end-cap faces. Figure 6 shows the nickel-plating on the end-cap with the sample holder screwed in.



Figure 6. Internal view of the nickel plating on the end-cap face with the sample holder screwed in.

3.1.2 Sample Holder

During the design and implementation of SB-IV, two sample holders were designed and machined. Both sample holders were custom-made, modified 2 in hex head bolts machined out of 2.5 in diameter 17-4 PH stainless steel bar stock. The original bolt modifications included the incorporation of face-sealing O-rings, a port for the copper lead, a groove to hold the sample, and a metal ground eyelet for Ni-Chrome wire ignition. Two face-sealing O-rings were incorporated, both 0.12 in wide and 0.08 in deep with inner diameters of 1 and 1.5 in. A small 0.25 in diameter hole was bored 0.24 in deep at the tip of the bolt to hold samples during testing. On one side of this hole, a small 6-32 UNC hole was tapped to accept a small eyelet used for grounding. A 0.1875 in hole leading to a $\frac{3}{4}$ "-16 UNF thread (at the hex head) was drilled on the other side. This fitting was used to admit a 24-gage copper wire sealed in a high-pressure compression seal gland from Conax (HPPL-24-A2), which served as the positive lead. The threads were 1"-8 UNC, 1 in deep. Unfortunately, during the initial pressure testing, the threads seized, and the hex head of this bolt sheared off while attempting to remove it. As a result, a secondary, slightly different bolt was machined.

As mentioned above, both sample holders were modified 2 in hex head bolts made of 17-4 PH stainless steel. The primary differences between the first and second sample holders are the O-ring grooves and the threads; all other ports remained the same. The diameter of the hole for the copper lead wire was also decreased to prevent deformation at high pressures. Instead of two face-sealing O-ring grooves, the second bolt only included the 1.5 in diameter O-ring groove. This additional feature was due to

the increase in thread diameter. When the original bolt broke, the hex head sheared off, leaving the remainder in the end-cap as seen in Figure 7. As a result, the remaining bolt had to be drilled out of the end-cap; hence increasing the bolt thread diameter and eliminating room for the 1 in O-ring. The new threads used on the sample holder are 1-16"-12 UNC threads. The threads were also changed to finer threads to prevent further seizing. Finer threads have less contact surface area, hence fewer areas to seize. Figure 8 shows the second sample holder. In addition to the face-sealing O-ring, the bolt threads are wrapped in Teflon tape for further sealing.



Figure 7. Original sample holder with the head sheared off and the remaining portion still in the end-cap.



Figure 8. Second sample holder.

3.1.3 Engineering Analysis

After the dimensions were finalized, calculations were performed to assure that the maximum allowable stress was not violated. If any stress calculation exceeded this allowable stress, structural integrity would be compromised. The primary calculated stresses were the circumferential, the tangential, the discontinuity or shell-to-end-cap junction, and the end-cap bending stresses as summarized in Table 3. As an additional safety measure, the total energy of explosion for SB-IV if it was pressurized at its maximum working pressure of 10,000 psi was also calculated. Should SB-IV fail and explode when pressurized at 10,000 psi, energy equivalent to 0.2 lb of TNT would be released.

Table 3. Calculated stress values and corresponding locations.

Stress	Location	Units	Values	Satisfied Allowable Limit
Allowable	-	ksi	27.50	-
Hoop	Shell	ksi	24.61	✓
Radial	Shell	ksi	15.00	✓
Allowable Shear	-	ksi	21.75	✓
Shear	End-cap Threads	ksi	0.65	✓
Shear	Bolt Threads	ksi	0.53	✓

When performing the heating and cooling tests, the strand burner will be exposed to temperatures as low as -88°F and as high as 200° F for roughly twelve hours at a time. The mechanical properties of 17-4PH change very little, roughly a 2% decrease in yield strength when exposed to 200°F for several hours. The maximum allowable stress becomes 26.95 ksi, which still satisfies the allowable limits for all stresses. For lower temperatures, the strength does not change, so the maximum allowable stress remains the same and all allowable limits are satisfied.

Since the design of SB-IV was based on SB-II, a comparative analysis was performed to validate the stress calculations. SB-II is rated to 5,000 psi with a design pressure of 8,000 psi (for more information, see Carro et. al)¹⁶. Since it was first built, SB-II has been extensively tested between pressures of 500-5,000 psi without failure. Therefore, the expected stresses between SB-II and SB-IV were compared along with their maximum allowable stresses.

SB-IV has a higher maximum allowable stress due to the material change. It should also be noted that while the allowable stress for SB-II was calculated with the ultimate tensile strength, the yield strength was used for SB-IV since it was the lower of the two values. If the ultimate tensile strength were used, the maximum allowable stress would be even higher. As for the hoop and radial stresses, the hoop stress only increases by eighteen percent, which is slightly higher than the increase in maximum allowable stress. However, as previously mentioned, the calculations for the new strand burner were made with the yield strength whereas the stress calculations for the current strand burner used the tensile strength. When compared using the tensile strength as the maximum allowable stress, the percent increase is actually 57.9%, which can more than handle the increase in hoop stress. The maximum radial stress is merely the design pressure. It should also be noted that while the endcap threads did not change, the bolt threads were changed to 1-12 UNC to increase the surface area and therefore decrease the shear stress. The comparison results are shown in Table 4. Additionally, Figure 9 and Figure 10 show comparative pictures of SB-II and SB-IV.

Table 4. Comparison of SB-IV to SB-II.

Stress	Location	Units	SB-II	SB-IV	% Increase
Allowable	-	ksi	23.75	27.50	15.79
Hoop	Shell	ksi	20.80	24.61	18.32
Radial	Shell	ksi	8.00	15.00	87.50
Shear	End-cap Threads	ksi	0.42	0.65	54.76
Shear	Bolt Threads	ksi	0.22	0.53	134

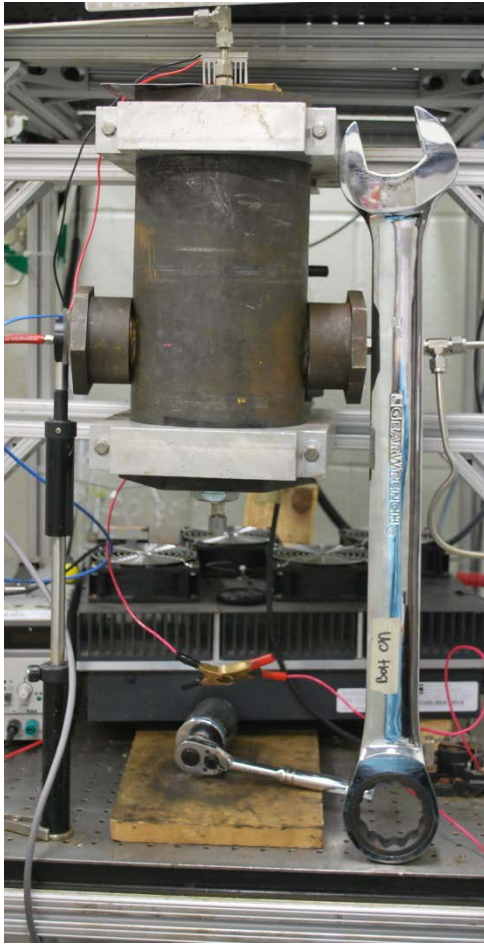


Figure 9. Vertically assembled SB-II.

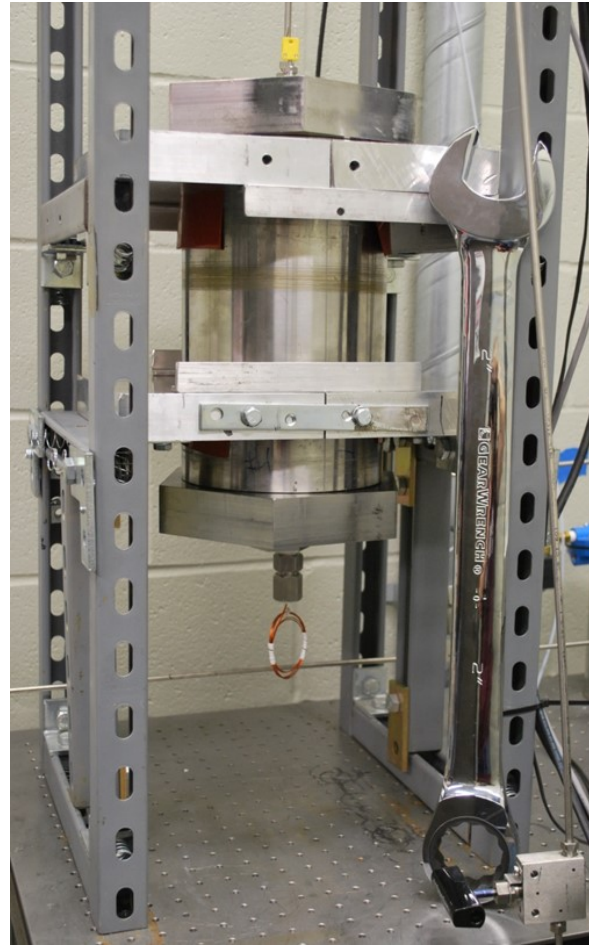


Figure 10. Vertically assembled SB-IV.

3.2 Facility Hardware

To mimic the combustion chamber pressure conditions of a rocket motor, the strand burner is pressurized with a chemically inert gas. For this study, high-pressure Nitrogen was supplied by two regulated, 6,000 psi, 570 ft³ bottles via 7,500 psi rated 0.25 in stainless steel (Swagelok) tubing. Nitrogen was chosen after performing a cost analysis comparing Nitrogen and Argon. Crawford et. al. found no significant difference in burning rate when using various inert gases⁶. The Nitrogen is also used pre- and post-

testing to purge the vessel of any lingering combustion gases or air. Figure 11 shows the Nitrogen bottles used for filling along with the light outside the test cell indicating a test in progress.

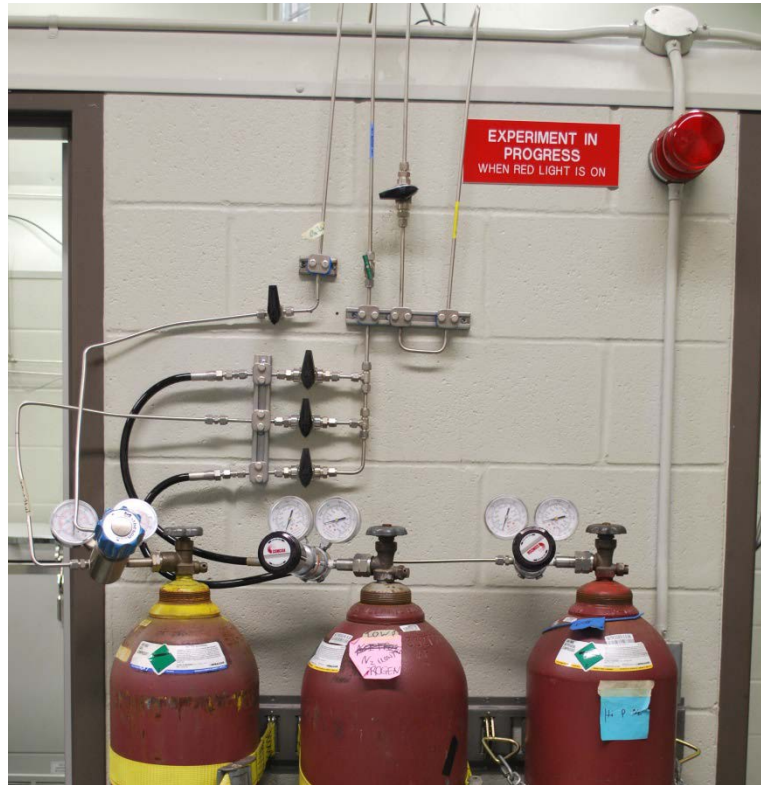


Figure 11. Nitrogen bottles used to fill and purge vessel before and after tests.

All testing was performed via a new remote-access control panel. The control panel is used to remotely fill and vent the strand burner, trigger ignition, and regulate the air supply to the gas booster. Figure 12 shows the new and existing control panels. The new control panel for SB-IV is pictured on the right and includes switches for the fill and exhaust valves along with the gas booster and ignition. It also has two DP41-E model digital readers, one for the test pressure and the other for the calibration pressure.

Both filling and venting are executed remotely by actuating solenoid-operated, normally closed pneumatic valves. The fill valve is a mini-hippo piston air operator rated to 6,000 psi from HiP. Since the fill valve is before the gas booster, a minimum pressure rating of 10,000 psi was not required. The exhaust valve however, is located after the gas booster so it must be rated for the working pressure of 10,000 psi. As a result, the exhaust pneumatic valve is a Hipco Diaphragm Air Operator rated to 10,000 psi also from HiP. Both pneumatic valves are air-operated, with the air supply connected to the shop air as shown in Figure 13 and Figure 14.



Figure 12. New (right) and existing (left) control panels for remote operation during experiments.



Figure 13. Mini-Hippo air piston used as the fill pneumatic valve.



Figure 14. Hipco diaphragm air operator used as the exhaust pneumatic valve.

Since Nitrogen only comes in bottles of a maximum 6000 psi, an air-supplied Haskel AG-75 gas booster was used to compress the fill gas to higher pressures. Using a minimum air supply pressure of 250 psi, the gas booster can compress the incoming Nitrogen to a maximum of 11,250 psi. An air compressor purchased for this project supplies the air. To avoid over-pressurization, the air supplied to the gas booster is controlled remotely via a solenoid valve attached to the line. Figure 15 and Figure 16 show the gas booster and air compressor, respectively.



Figure 15. Gas booster used to compress the incoming Nitrogen to pressures above 6,000 psi.



Figure 16. Air compressor used to supply air to the gas booster.

The existing plumbing in the test cell was only rated to 7,500 psi, so all new, 20,000 psi-rated medium pressure tubing was installed past the gas booster for the high-pressure system. Since only the line beyond the output of the gas booster experiences pressures above 7,500 psi, only these portions used the medium pressure line. The fill line connects to the existing line going to the Nitrogen tanks via a T-Junction. For safety reasons, there are several manual exhaust valves. As shown in Figure 11, there are two manual ON/OFF quarter turn ball valves located after each Nitrogen tank regulator along with a needle valve that sets the fill rate. There are also two emergency exhaust valves, located before and after the gas booster. To switch between the hot and cold temperature experimental setups, there are two additional quarter turn ball valves, one leading to the vertical setup used for high pressure and hot temperature experiments, and the other to

the freezer for low-temperature tests. Figure 17 displays a schematic of the plumbing, while Figure 18 shows the actual experimental setup.

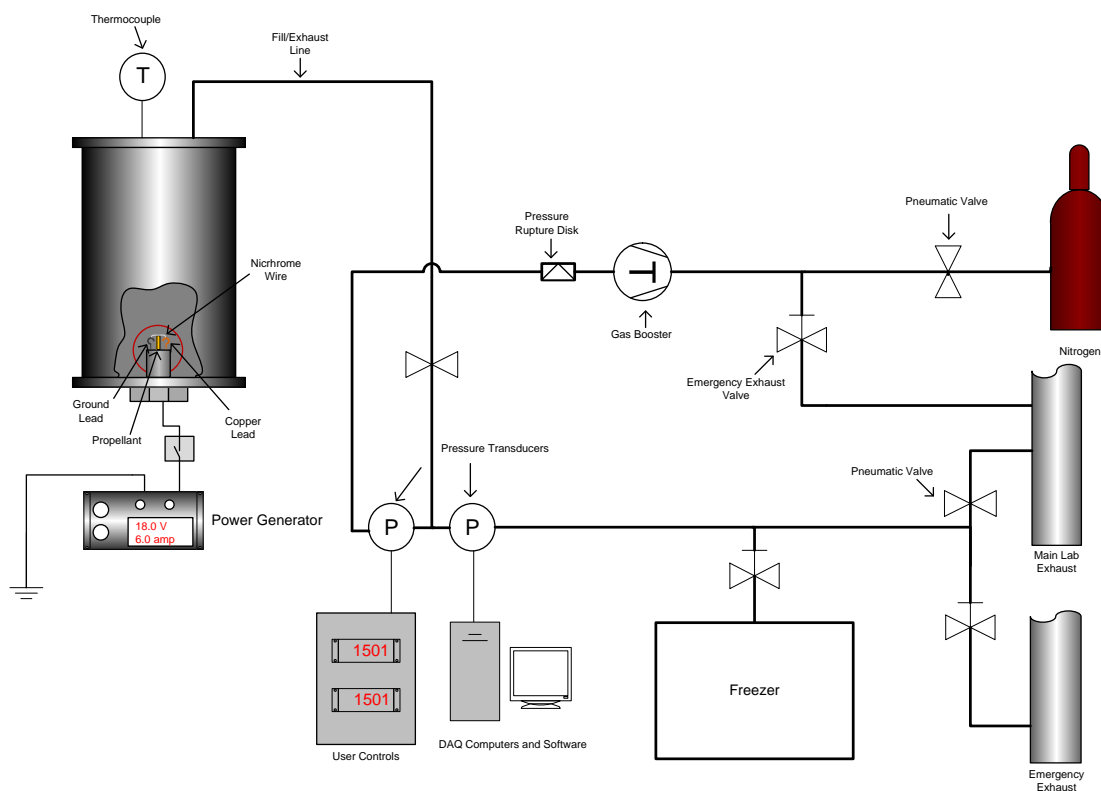


Figure 17. Plumbing schematic of experimental setup.

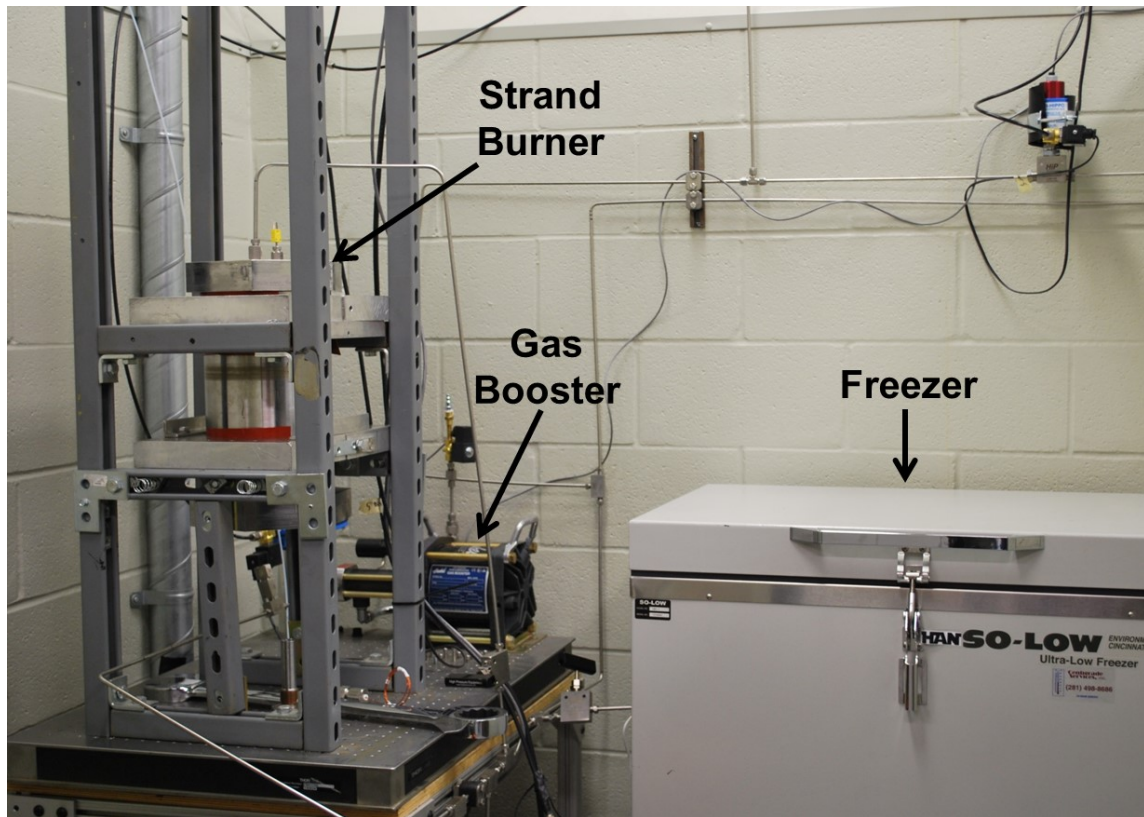


Figure 18. New experimental setup for high pressure and temperature sensitivity experiments.

Two pressure transducers are located after the gas booster before the quarter turn valves leading to the two experimental setups. One is connected to GageScope for recording the pressure during the test, while the other is used to determine the vessel pressure while filling. Due to project time constraints, both pressure transducers are PX02 series rated to 40,000 psi from Omega with a 0-5 V output. Unfortunately, at the time the pressure transducers were ordered, all of the PX02 series pressure transducers rated between 10,000 and 30,000 psi were out of stock. Since these pressure transducers are rated to a much higher than the working pressure for this project, there will be more noise in the pressure trace collected by GageScope. However, as shown in a later

section, the beginning and end of the burning rate are still clearly defined when observing the pressure trace. The pressure transducers and quarter turn valve leading to the high-pressure setup are shown in Figure 19.

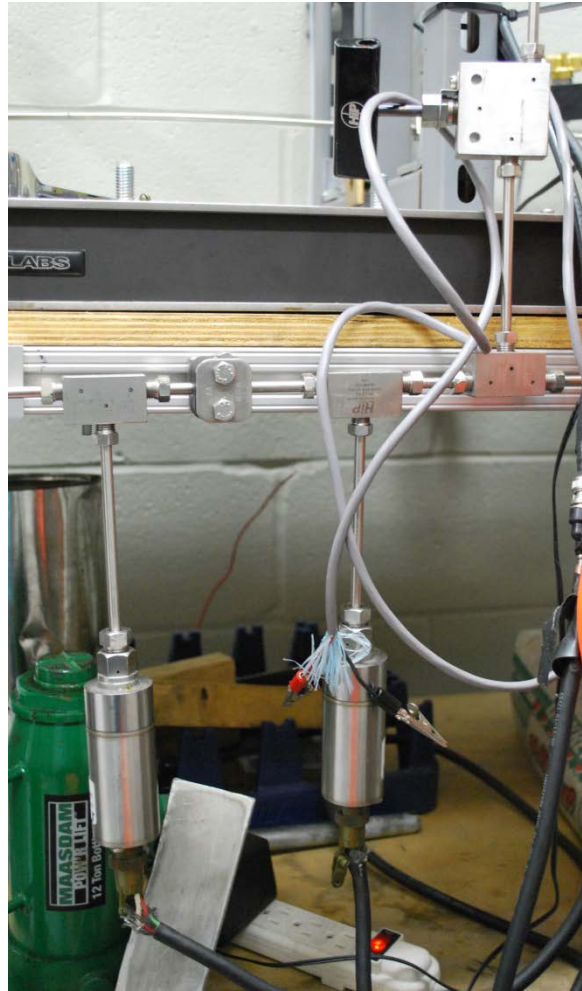


Figure 19. Pressure transducers and quarter turn valve connecting to the vertical setup used for high pressure and high-temperature tests.

For the temperature sensitivity tests, a thermocouple was placed inside the strand burner via a port in the fill end-cap as previously described and shown in Figure 10. The

thermocouple used is a K-type thermocouple from Conax designed for pressures up to 20,000 psi. The temperature is then monitored and recorded during the burn using a FLUKE thermometer as shown in Figure 20. For high-pressure temperature tests where knowing the temperature during the experiment is not vital, the thermocouple is replaced by a cap. This exchange protects the thermocouple from unnecessary exposure to combustion products. A view of the fill end-cap with the cap in place of the thermocouple is shown in Figure 21.



Figure 20. FLUKE thermometer used to monitor and record the temperature detected by the thermocouple located inside the vessel.



Figure 21. Thermocouple port with cap in place of thermocouple for high-pressure testing.

3.3 Testing Procedures

3.3.1 Burning Rates

All propellant samples are approximately 1 in in length with a diameter of 0.1875 in. They are manufactured in the test facility by the Petersen Group at Texas A&M University using techniques developed by Stephens et al.³⁰. The burning rates were determined using the burn time as indicated by the clear inflection points from the measured pressure trace indicating the start and end of combustion and initial propellant strand length. An example pressure and light trace for SB-II is shown in Figure 22. Although SB-IV has no optical ports, thus no light trace, the pressure traces recorded are similar to those using SB-II as proven through the subsequent characterization testing. It is still evident when the ignition begins and when the burn finishes. Ignition was

achieved by running a current across a Nichrome wire attached to two metal leads.

Figure 23 shows a sample propellant loaded in the second new sample holder with a Nichrome wire attached to both metal leads. A detailed description of this method can be found in Stephens et al.³.

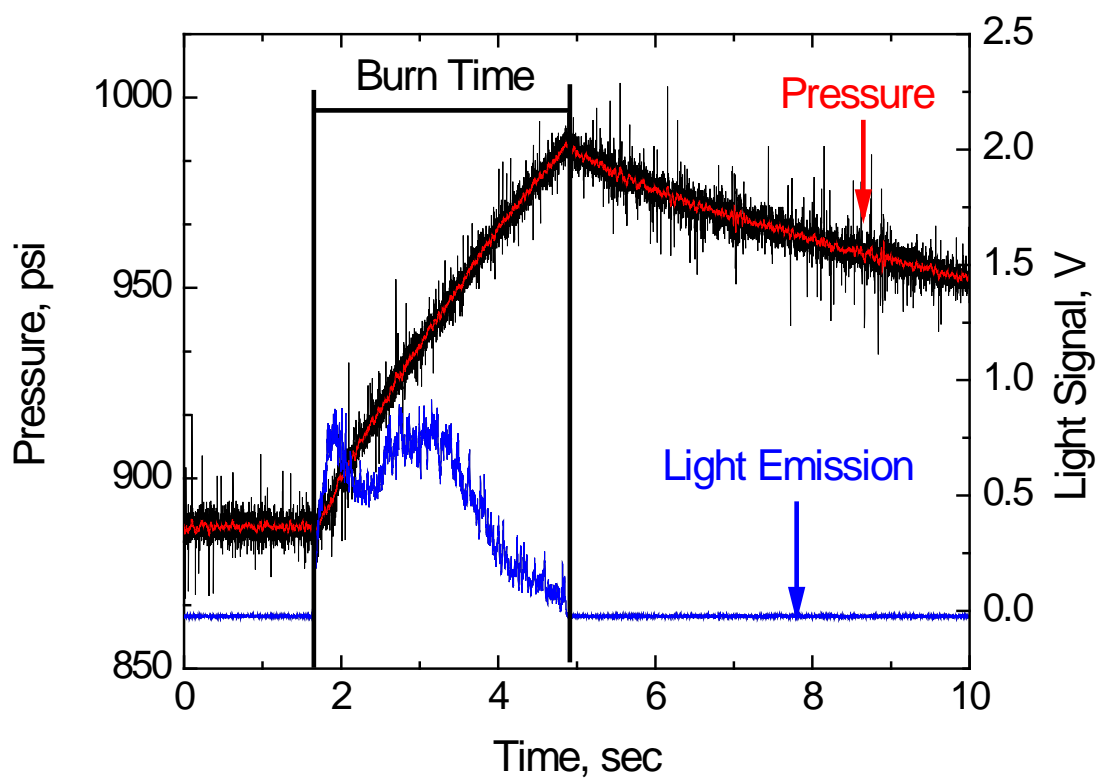


Figure 22. Sample pressure and light-emission data plot taken from experiments using SB-II.



Figure 23. Example loading of propellant sample in the modified bolt using Nichrome wire ignition.

3.3.2 Temperature Sensitivity

Temperature sensitivity (σ_p) is calculated by measuring burning rates at 3 different temperatures, -88 °F, 70 °F, and 194 °F, over a range of pressures. The -88°F burning rates are measured by placing the strand burner horizontally into a So-Low freezer as seen in Figure 24. The temperature of the freezer is controlled through a panel located on the front as shown in Figure 25. For both the low- and high-temperature tests, the test vessel required a minimum of 8 hours to reach the desired initial temperature. The sample holder is loaded while cooling and heating to ensure constant expansion and

contraction of the material. Additionally, several large pieces of scrap metal are placed into the freezer prior to the strand burner to act as heat sinks. Otherwise, the freezer is overloaded and cannot maintain the desired temperature.

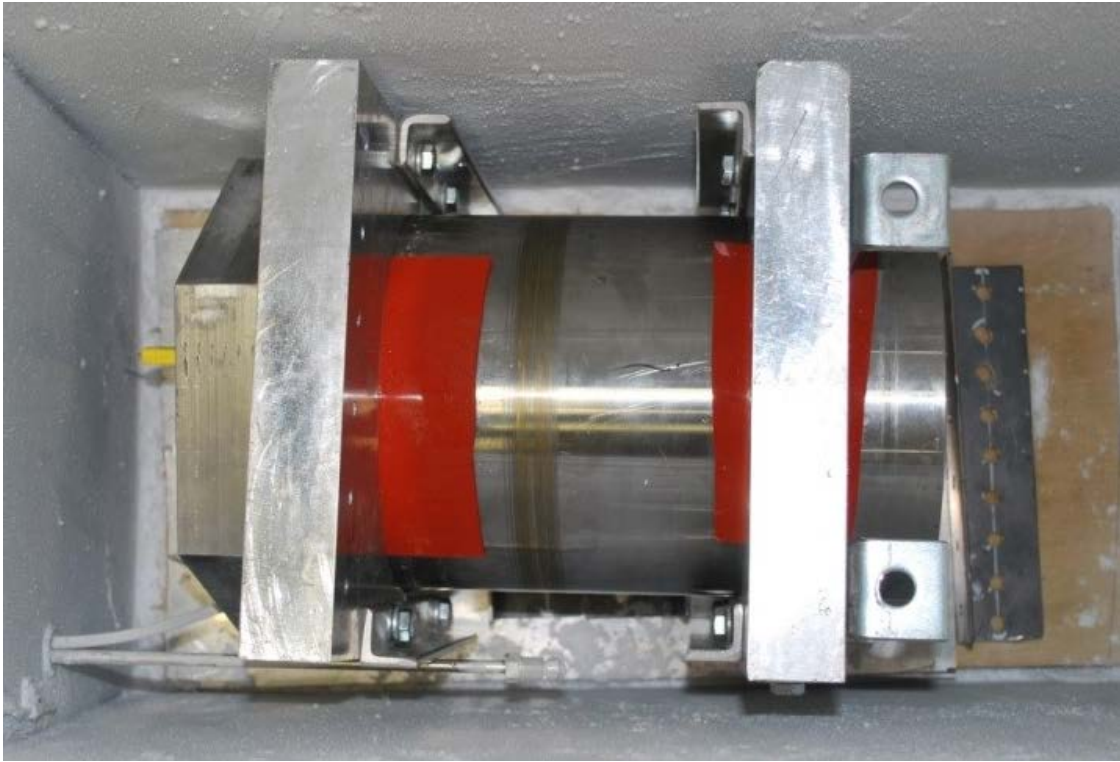


Figure 24. SB-IV placed into the freezer for low-temperature sensitivity tests.

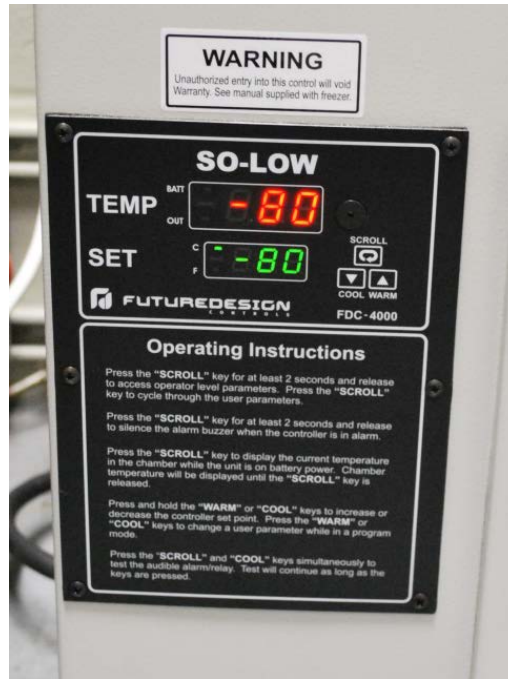


Figure 25. Freezer control panel used to set the freezer temperature.

The 194°F burning rates are measured by wrapping the strand burner in heating tape and insulation as seen in Figure 26. The heating tape was powered by a controller with a thermal feedback sensor. To regulate the temperature, a k-type thermocouple was placed in the space between the bottom end cap and the wall of the strand burner. From the temperature measurement, the heating tape controller determined the appropriate output power to maintain the programmed temperature.



Figure 26. Heating tape wrapped around SB-IV for high-temperature sensitivity tests. The same vertical mount is used for high-pressure testing.

For both hot and cold temperature sensitivity tests, the strand burner was purged with nitrogen prior to testing. The temperature was monitored using a thermocouple inserted in the top of the strand burner as previously described. During the purging process, the temperature would rise during filling. The temperature would fall back to the temperature indicated by the thermocouple prior to the filling process. Once the temperature stabilized at the desired temperature, the strand was ignited using the Nichrome wire. The propellants were burned horizontally for the low-temperature tests

due to the confined space in the freezer, while the samples were mounted vertically for heating tests due to the propellants becoming softer when heated. Past studies have shown no significant difference between burning rates when burned horizontally or vertically.

3.4 Characterization

3.4.1 Pressure Transducer Calibration

As described before, the primary method for determining the burning rate of varying propellant formulations is measuring the transient pressure increase during combustion. The first pressure transducer located before the quarter turn valves is used in conjunction with GageScope to record this increase. Both pressure transducers offer accuracies of 0.15% FS (linearity, hysteresis, repeatability) throughout their pressure range up to 40,000 psi. The signal from the first pressure transducer is acquired and recorded on the same Data Acquisition System (DAS) via a dual-channel waveform digitizer PCI bus-based card and its corresponding software from Gage Applied Technologies as described thoroughly in Carro et al.¹⁶. To switch between SB-II and SB-IV, the pressure transducer connection to GageScope is simply swapped accordingly. While this limits the overall testing capabilities since both strand burners cannot be simultaneously operated, it is more economical and efficient since the data acquisition system is already in place and well-documented. The second pressure transducer located before the quarter turn valves, as seen in Figure 17, is used to determine the ‘real time’ pressure inside the vessel. The pressure is then displayed on a digital reader on the

control panel. This digital readout allows the operator to know when the desired test pressure is obtained to avoid over-pressurization and wasting Nitrogen. Similarly, this display is used post-test to verify complete venting of the system.

In addition to the calibrations performed by the manufacturers, both of the new pressure transducers were calibrated using the existing SB-II pressure transducers. To calibrate the pressure transducers, both the fill lines to SB-II and SB-IV were opened and filled to various pressures. The output signal from the new pressure transducer to GageScope was then compared to the pressure displayed on the existing control panel. A set of six different pressures ranging from 0 to 3685 psi were then used to generate the linear calibration curve shown in Figure 27. The equation for the generated trend line is then put into Origin plotting software to convert the recorded voltages during the propellant burns to pressures.

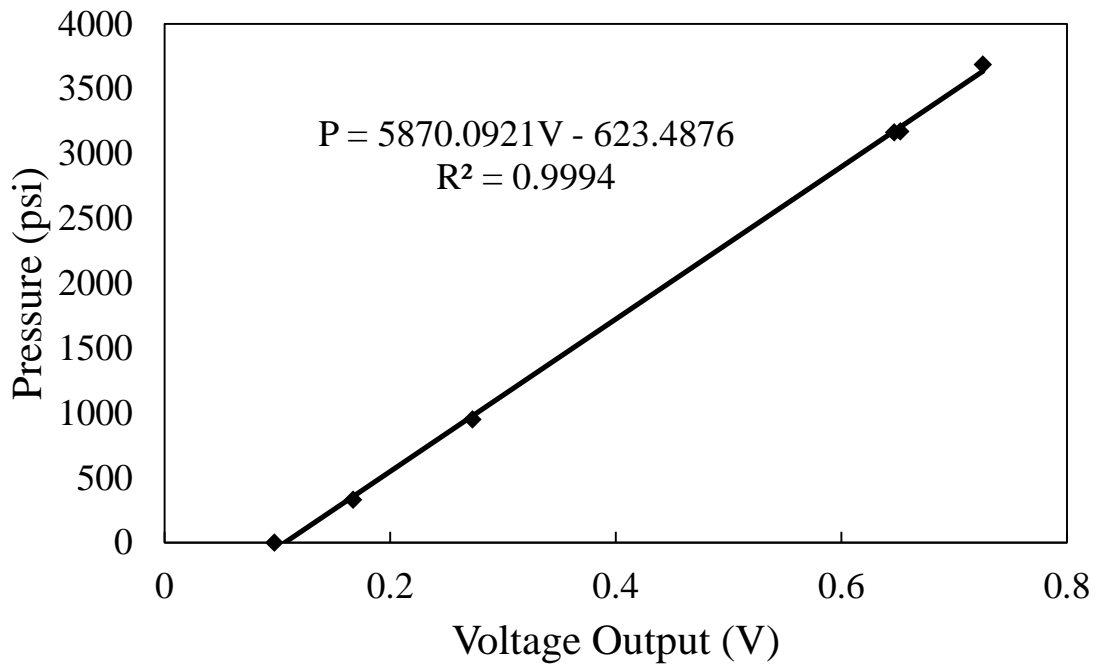


Figure 27. Pressure calibration for the new GageScope pressure transducer using the existing system.

Similarly, for the second pressure transducer, the output voltages displayed on the new digital reader were recorded along with the corresponding values from the existing system for a set of four pressures ranging from 0 to 3688 psi. These values were then plotted and used to generate the relationship displayed in Figure 28 between pressure and voltage output. The resulting equation was then used to convert the voltage output displayed to pressure to determine the ‘real time’ pressure inside SB-IV.

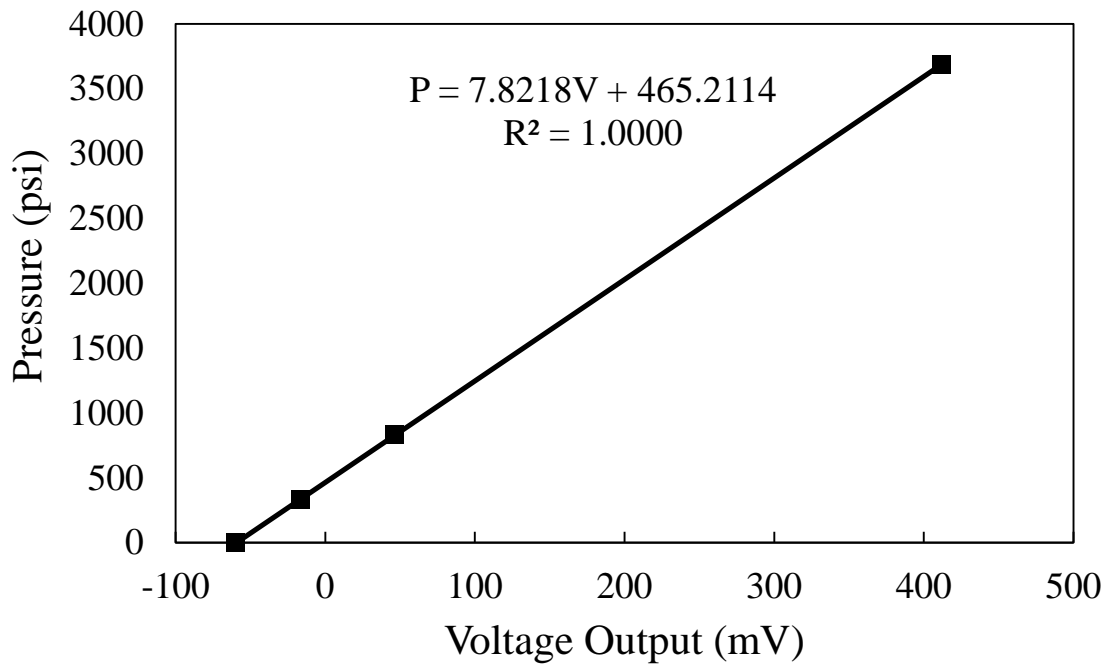


Figure 28. Calibration for the pressure transducer used to measure 'real time' vessel pressure using the existing system.

3.4.2 Comparison to SB-II

Along with calibrating the pressure transducers, historical data collected using SB-II was used to verify the burning rates in the new high-pressure strand burner. Three primary formulations, as summarized in Table 5, were used to verify the results in the new SB-IV. Several 80% monomodal AP/HTPB composite propellants were burned in SB-IV during preliminary pressure testing. These preliminary data were used to verify the burning rates and pressure increase in SB-IV against past historical data collected using SB-II. Base-01 was used to verify that the burning rate data collected in the new high-pressure strand burner are consistent with those collected in SB-II. The comparative results are shown in Figure 29. The black data points and trend line were

generated using the existing test vessel, SB-II, and the red data points are those collected in SB-IV. While the entire formulation falls slightly below the historical baseline trend line, the new points collected in SB-IV fall within the scatter of those collected in SB-II, hence validating the burning rates measured in the new strand burner.

Table 5. Propellant formulations used in characterization tests for the new high-pressure strand burner.

Batch	AP Distribution	AP Particle Size (μm)
Base-01	80% Monomodal	200
Base-02	80% Monomodal	200
Base-03	80% Monomodal	138

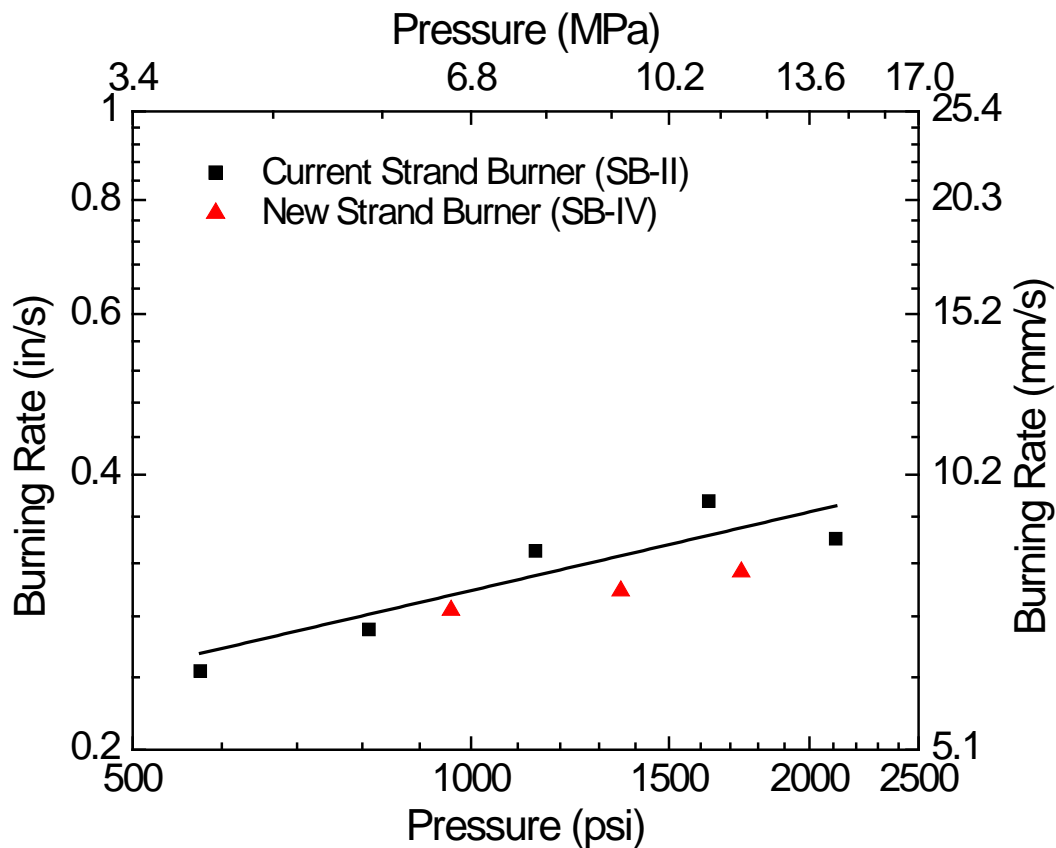


Figure 29. Burning rate data collected using both SB-II and SB-IV for an 80% monomodal propellant batch with an average AP particle size of 200 μ m.

The pressure increase was also verified while collecting preliminary burning rate data using the new strand burner. Since the volumes of SB-II and SB-IV are the same, they should also generate similar pressure increases during propellant burns for the same average test pressure. Figure 30 and Figure 31 show example pressure traces recorded using SB-II and SB-IV, respectively. The pressure traces are for the same 80% monomodal baseline formulation (Bases 01 and 02 in Table 5. Propellant formulations used in characterization tests for the new high-pressure strand burner.) and similar average test pressures of 1767 psi and 1739 psi, respectively. Observing the pressure

risers in Figure 30 and Figure 31, it is seen that the pressure increases roughly 200 psi for both propellant burns. What appears to be a spike in pressure in Figure 31 is actually a voltage spike from the ignition button. During preliminary testing, whenever the ignition button was pushed, the DAS would detect the voltage spike from the initial completion of the circuit used to initiate combustion. Subsequently, when the recorded voltage output was copied over to Origin and converted to pressures, this voltage spike would appear as a pressure spike, when in reality, it is purely a voltage spike due to ignition. This problem was resolved in later tests.

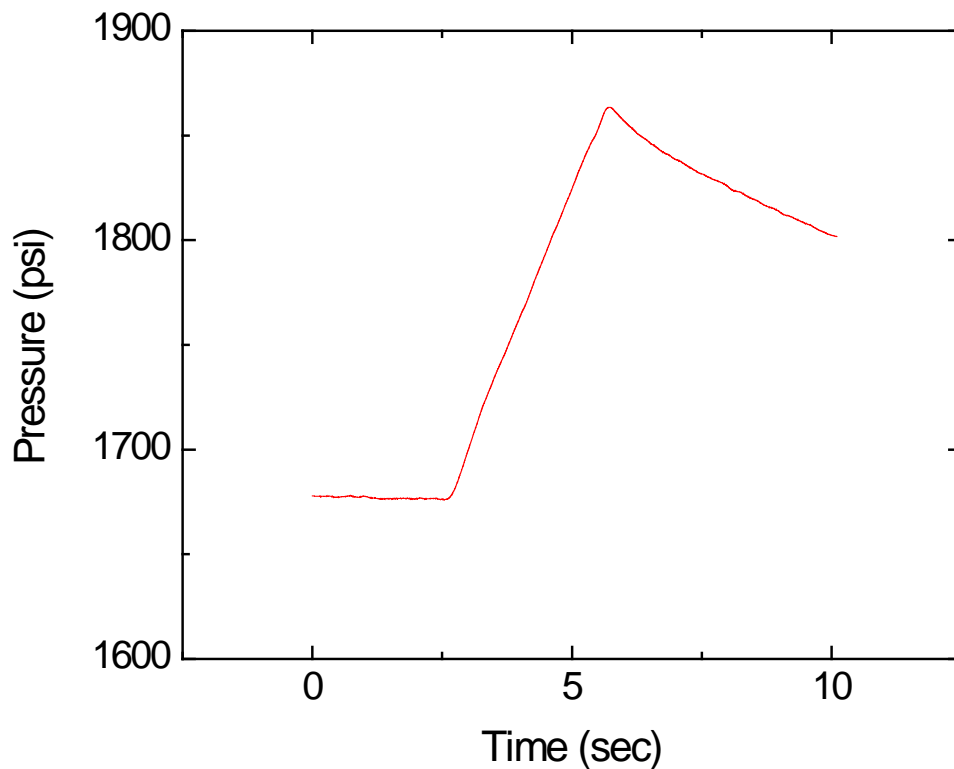


Figure 30. Example pressure trace collected using SB-II for an 80% monomodal propellant, average AP particle size of 200 μm , at an average test pressure of 1767 psi.

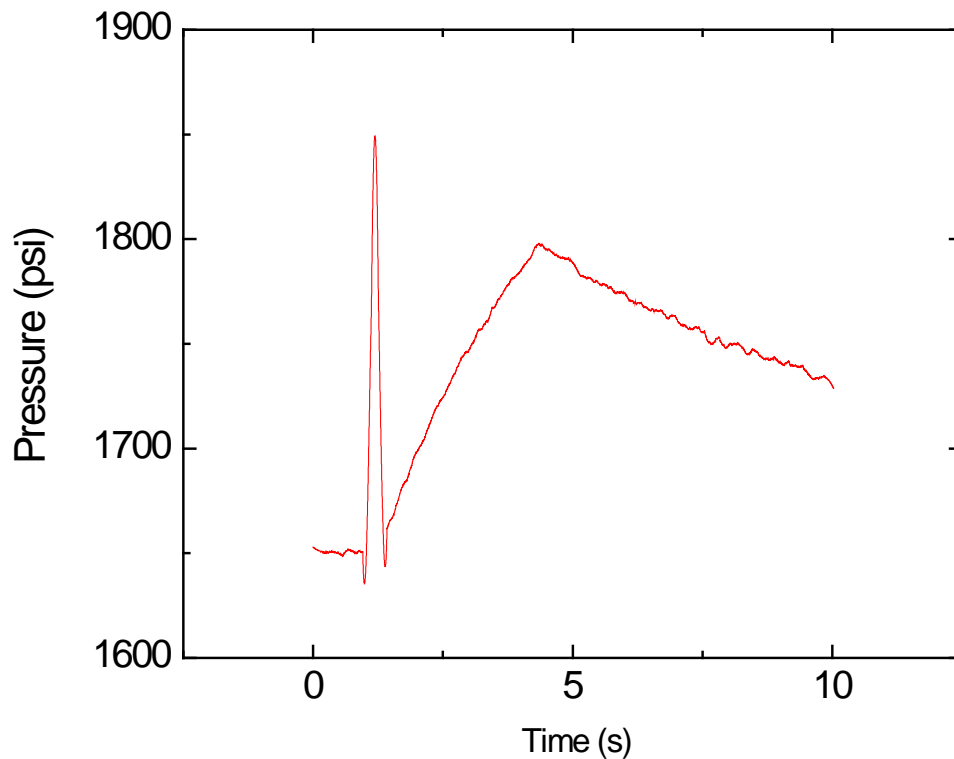


Figure 31. Example pressure trace collected using SB-IV during preliminary pressure testing for an 80% monomodal propellant, average AP particle size of 200 μm , at an average test pressure of 1739 psi.

3.4.3 High-Pressure Results

Once the preliminary burning rates and pressure rises for the new strand burner were validated, higher pressures were tested to verify the design capabilities. To reach the higher pressures, the test vessel was first pressurized to the maximum pressure left in the Nitrogen tank. The gas booster was then turned on and left on until the desired test pressure was reached. It was discovered during initial testing that to reach pressures above 6,000 psi, almost an entire tank of Nitrogen was first needed to pressurize the

vessel before turning on the gas booster. The gas booster required a minimum of 150 psi to boost the Nitrogen to higher pressures. As a result, the air compressor used to supply air to the booster had to run constantly during testing to maintain its maximum capacity of 150 psi. It was also discovered during pressure testing that the O-rings located on both end-caps did not seal properly, resulting in a significant leak rate as seen on the example pressure trace in Figure 32. Consequentially, the strand burner had a difficult time maintaining constant, high pressures and ultimately could reach pressures above 8000 psi. The strand burner itself did not fail, but rather the O-rings used to seal internally between the end-caps and main body. Further details are described in Section 4. The pressures that were reached however resulted in burning rates that followed the previously established trend for Base 03 shown in Figure 33.

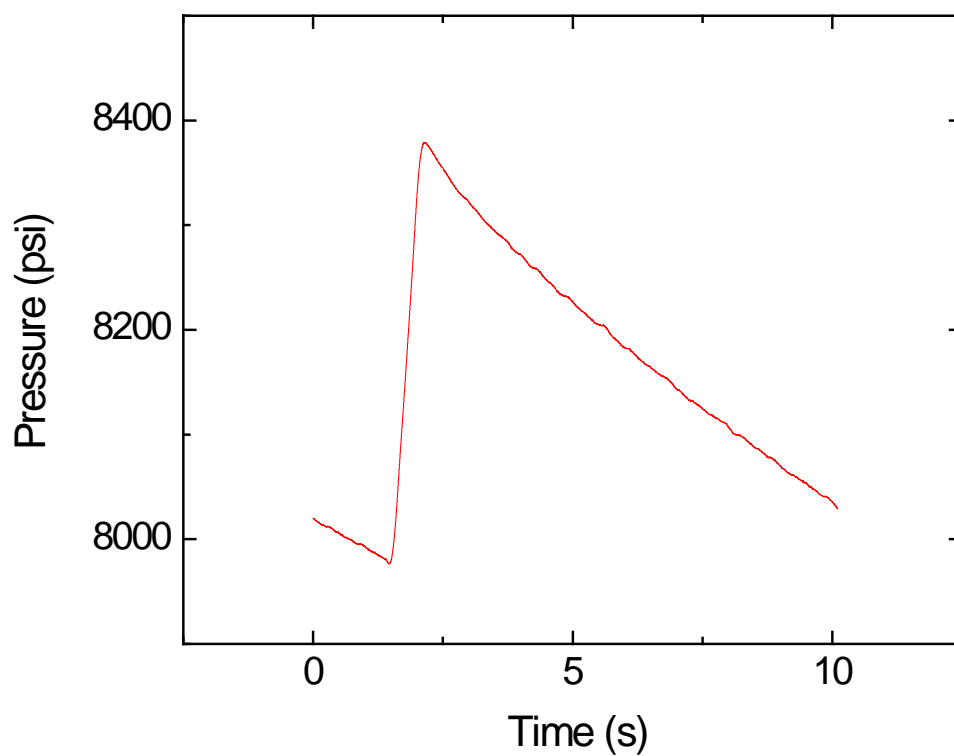


Figure 32. Example pressure trace collected using SB-IV for an 80% monomodal propellant, average AP particle size of 138 μ m, at an average test pressure of 8193 psi.

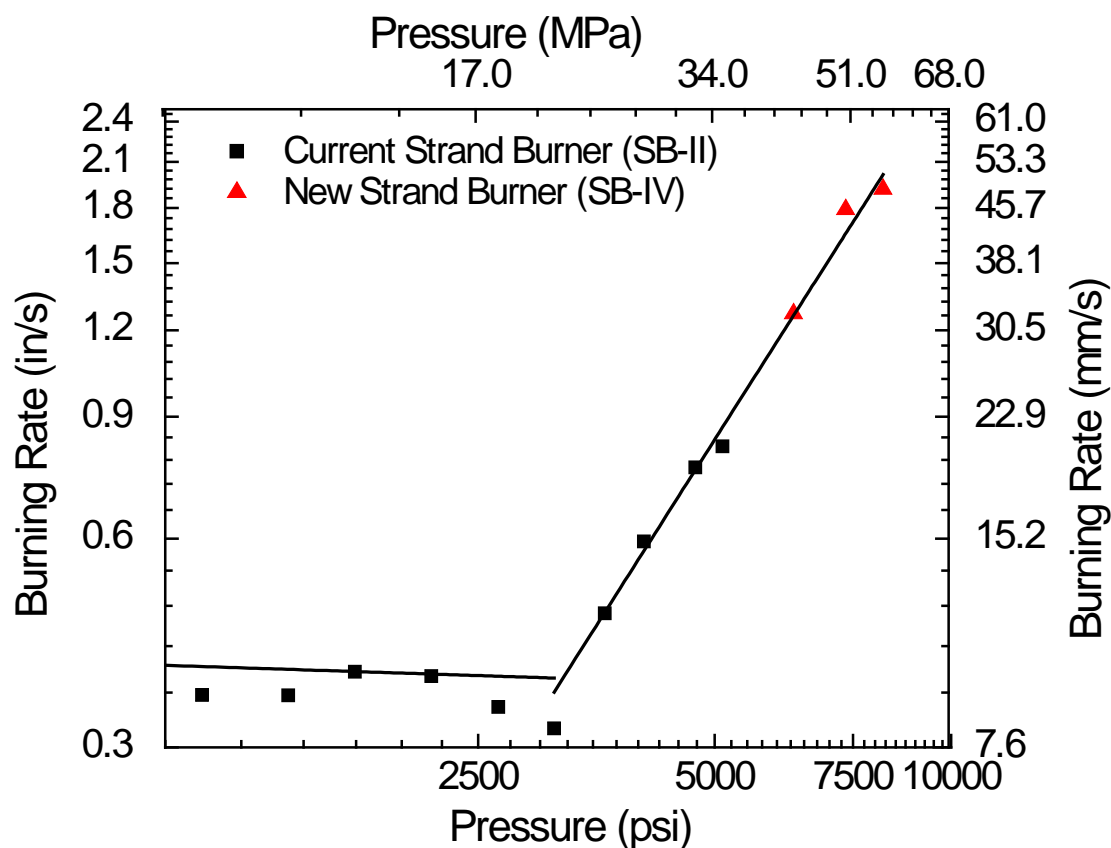


Figure 33. High pressure burning rate data collected using the new SB-IV for an 80% monomodal propellant with an average AP size of 138 μ m (Base 03).

3.4.4 Temperature Sensitivity Results

To test the temperature capabilities of the new strand burner, both low- and high-temperature sensitivity tests were performed using the Base-03 formulation as seen in Table 5. The low-temperature tests were performed first by placing the entire strand burner into the freezer as pictured in Figure 24 and letting it cool for a minimum of eight hours until it reached the desired initial temperature of -88°F. The samples were also placed in the freezer for a short period to cool them to an initial temperature of -88°F. One sample was tested at the low temperatures and two at the high temperatures. For the

high-temperature tests, the strand burner was wrapped in heating tape and heated to an initial temperature of 194°F. The burning rate results for both tests are shown in Figure 34. Similar to Demko et al.'s results shown in Figure 1, the propellants burned at the high initial temperature have higher burning rates than those at ambient temperature, while the propellants burned in the cold environment are lower. Only one pressure was tested to obtain a direct comparison. The temperature sensitivity values are also tabulated in Table 6 and compared to the results of Demko et al.²⁰. It should be noted that although the formulations used in this temperature sensitivity study and in Demko et al. were the same, the average AP particle sizes were different. Additionally, although it appears the data presented in this study contradict those in the previous literature review, it should be noted that the aforementioned studies used pure AP or pressed AP pellets, while this study and Demko et al. used AP/HTPB composite propellants.

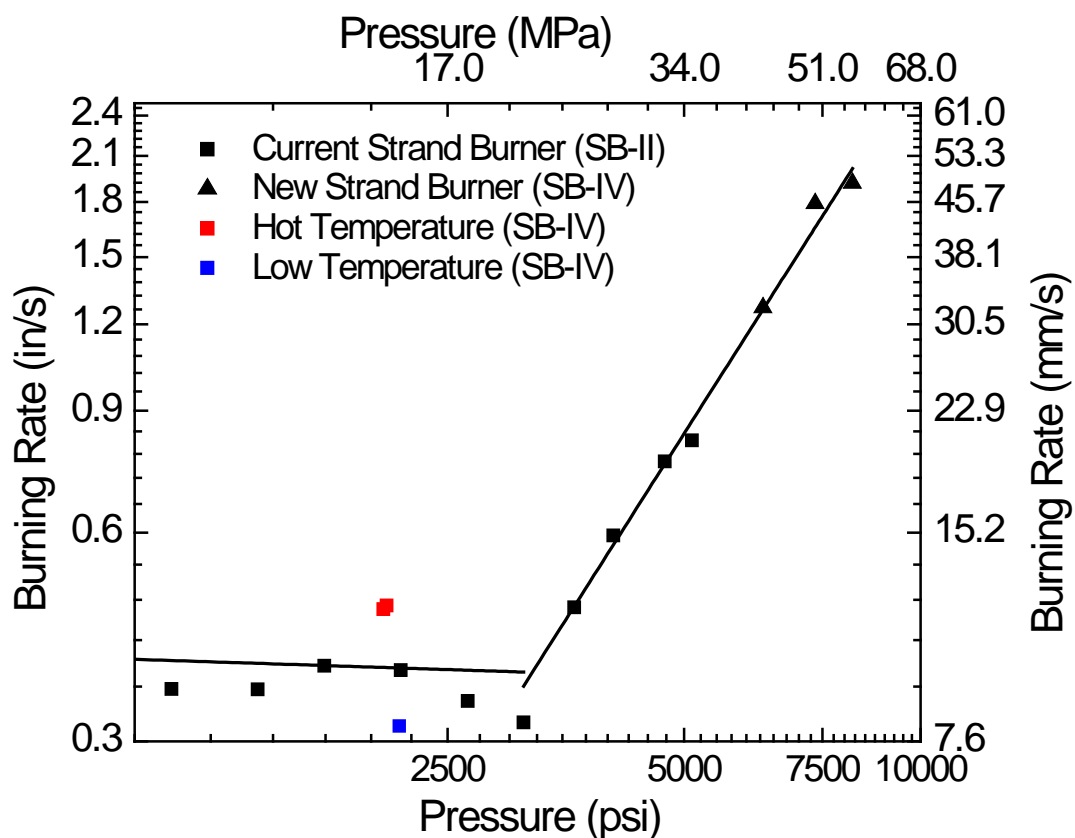


Figure 34. Example temperature sensitivity data collected using the new high pressure strand burner for an 80% monomodal propellant with an average AP particle size of 138 μm .

Table 6. Comparative temperature sensitivity data for 80% monomodal propellants using SB-II and SB-IV.

Mix	AP Particle Size	Hot σ_P (%/K)	Cold σ_P (%/K)	Average σ_P (%/K)
Demko et al. ²⁰	200	0.34	0.70	0.49
Base-02	138	0.29	0.23	0.26

3.4.5 Uncertainty

As with all experiments, there is an inherent uncertainty when taking measurements. The uncertainty in burning rate constants comes from a variety of sources, primarily from natural combustion fluctuations, variabilities in mixture uniformity between batches, and measurements. To minimize the variations between batches, a minimum of ten samples are burned for each propellant mixture. The length and mass of each sample are measured to ensure uniform density. Discrepancies in density can account for larger-than-normal scatter in the measured burning rates. In addition to mass and length measurements, uncertainty also stems from instrumentation errors.

Total uncertainty from the pressure trace, sample length/mass, time resolution, and temperature measurements was calculated using the root-sum-square (RSS) method. The tolerances in length, mass, and temperature measurements were found to be ± 0.0005 in, ± 0.01 g, and $\pm 0.1^\circ\text{F}$, respectively. The uncertainty in the DAQ pressure transducer is 0.15% of the test pressure as reported by the manufacturer. This amounts to less than 1 psi (0.75 psi) at the minimum test pressure of 500 psi and 15 psi at the maximum, 10,000 psi. The uncertainty in burning rate time was determined from the recorded pressure trace. The largest source of uncertainty in the time measurement and ultimately, overall, comes from selecting the point of ignition. Unlike the end of the burn, where there is a distinct peak in the pressure rise, the beginning of the burn is much slower and not as clear. As seen in Figure 30, there is a slight curve, or transient portion, at the beginning of the pressure trace, making it difficult to select the exact point of ignition. Therefore,

the total uncertainty in the time measurement was taken as this initial transient portion as seen in Figure 35, which was about ± 0.47 seconds.

The overall total burning rate measurement uncertainty for this study ranged from 12.8% to 15.1%, compared to 4.3-9.1% using SB-II. This increase in uncertainty comes from the transient ignition portion of the pressure trace. As seen in Figure 31 and magnified in Figure 35, there is a sudden spike in the pressure trace resulting from the sudden increase in voltage due to the ignition circuit being completed. This spike increases the duration of the transient portion, causing the overall measurement uncertainty to increase. For example, the initial transient portion using SB-II (without the voltage spike) is approximately 0.16-0.25 seconds but almost double at 0.47 seconds using SB-IV (with the voltage spike). Although the overall uncertainty is between 12.8-15.1%, the actual burning rates typically fall within 10% scatter of the predicted burning rates using a best-fit trend line.

For temperature sensitivity measurements, the overall uncertainty remains the same since the majority of the uncertainty comes from the transient portion of the time measurement. The inclusion of the temperature measurement uncertainty is very small, $\pm 0.1^{\circ}\text{F}$; thus has little to no effect on the overall uncertainty. Additional sources of uncertainty can be attributed to human errors such as incorrect sidewall inhibitor application.

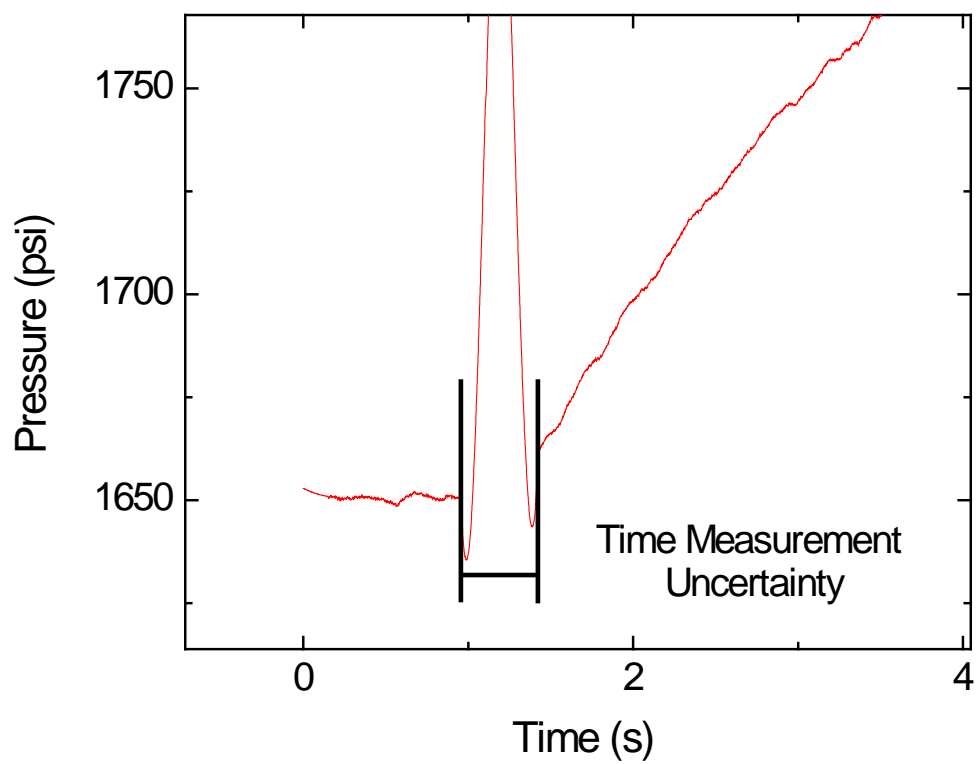


Figure 35. Example uncertainty in time measurement using SB-IV.

4. CONCLUSION

4.1 Summary

A new, very high-pressure facility was developed and characterized for studying the burning rates of propellants at extreme temperatures. The pressure testing capabilities of the author's lab were doubled to a working pressure of 10,000 psi. The new facility is also capable of determining propellant temperature sensitivity for temperatures ranging from -88°F to 194°F using a new So-Low Freezer and heating tape, respectively. The new strand burner design also incorporates a thermocouple so the initial internal pressure vessel can be monitored during burns. Additionally, all new tubing and fittings were installed along with fill and exhaust pneumatic valves to ensure a minimum pressure rating of 15,000 psi.

Burning rates were obtained from the pressure trace recorded in GageScope, while the temperature sensitivities were determined by raising and lowering the initial propellant temperature. The high-temperature sensitivity tests were performed by wrapping the strand burner in heating tape and allowing the entire vessel to reach the desired temperature. The low-temperature tests were achieved by placing the strand burner and bolt into a So-Low freezer and cooling it to the required temperature. The 'real time' vessel temperature was monitored via a thermocouple located inside the vessel. The gas inside the vessel was allowed to reach equilibrium after filling before burning the propellant. The resulting data were subsequently used to calculate temperature sensitivity.

The new strand burner was extensively characterized through a series of tests. To verify the burning rate and pressure increase, the same batch of propellants was burned in both the existing strand burner, SB-II and the new vessel, SB-IV. The resulting data showed similar burning rates and pressure rises, therefore confirming the new strand burner's accuracy. Similarly, temperature sensitivity data collected in the new strand burner were qualitatively compared to past studies to verify their validity. To verify the high-pressure testing capabilities of the new strand burner, tests were performed at pressures above 6,000 psi. While the strand burner was able to be pressurized up to 8,000 psi, the target working pressure of 10,000 psi was not reached at the time of this thesis due to sealing issues. As a result, recommendations are made in a following section to address this issue.

4.2 Challenges

Implementing the design of the high-pressure strand burner required "trouble shooting" in new territory. Although the basic design and machining were similar to the current strand burner employed by the Petersen Research Group at Texas A&M University, this latest vessel stretched material and operating parameters.

The increased scale produced challenges associated with imprecise machining. Initial, inaccurate machining was evident during the first pressure testing. The end caps and the bolt used for holding the propellant sample all suffered from thread galling at one point during initial testing and required either customized tool fabrication or additional machining. Galling between the vessel chamber and the end caps required re-

machining to remove excess metal and properly tighten each end cap. While the re-machining solved the galling problem, it introduced sealing issues between the end-caps and main body. The O-ring groove was altered during the re-machining, causing the originally chosen O-rings to not compress and seal properly. As a result, the strand burner could not consistently hold pressures above 7,000 psi and only reached a maximum pressure of 8,000 psi to date.

As mentioned in earlier sections, the propellant holder was also re-machined due to thread galling. A completely new bolt was machined along with the end-cap bolt port. To prevent galling in the future, the threads per inch were increased, making the contact surface area on each thread slightly smaller. Additionally, the wall thickness between the copper lead wire and threads was increased to prevent any deformation due to the high pressures. The new propellant holder has one face-sealing O-ring and holds pressure much better than the previous bolt.

O-ring materials also presented difficulties when testing at pressures above 7,500 psi. While O-rings are typically rated for temperature ranges and/or chemical resistance, their operating pressure limits are not supplied. The initial O-rings chosen had a chemically resistant outer casing with a silicone core. While they supplied the necessary chemical resistance and temperature range, the chemically inert outer casing failed at pressures above 7,500 psi, causing the O-ring to over-expand and burst. Coupled with the increased size of the vessel, removal of the end cap for O-ring replacement required unique servicing. As a result, the O-rings were changed to a more-rigid type without a chemically inert outer casing. Additionally, ignition and thermocouple wiring were

adjusted to ignite the propellants reliably and record the temperature of the gases in the vessel before and after combustion. All-new, 20,000 psi-rated tubing and fittings were also installed since the previous facility was only rated to 10,000 psi. A new gas booster and air compressor were both used to reach the higher pressures since tanks of Nitrogen only come at a maximum of 6,000 psi.

Transitioning between hot and cold temperature sensitivity testing required a portable crane to move the vessel (100 kg) between the vertical and horizontal set-ups. Large masses of metal were placed in the freezer prior to testing to act as heat sinks. For both sets of temperature sensitivity, the vessel required a minimum of eight hours to heat or cool to the desired temperature, then another 24 hours to reach room temperature before switching to the other temperature extreme. Similarly, the high-pressure (5000 to 10,000 psi) burning rate tests took approximately three times as long as the normal pressure range (500 to 4000 psi) to perform.

4.3 Recommendations

The only testing capability of the new strand burner not verified at the time of this thesis is the working pressure of 10,000 psi. It is evident by looking at the example pressure trace in Figure 32 that the new strand burner has a high leak rate. Even with a constant air supply to the gas booster, the gas booster cannot increase the pressure fast enough to overcome the leak rate. As a result, the current maximum working pressure is only 8,000 psi. To solve this problem, the author first recommends re-measuring each O-ring groove on the two end-caps. During preliminary testing, the end-cap threads galled,

causing the machinist to re-thread and machine down the circumferential O-ring grooves. Since these diameters changed, the original O-rings are now unable to completely compress, causing leaks where they should have sealed. Therefore, re-measuring the O-ring grooves and choosing new O-rings based on the guidelines in the Parker Handbook for O-rings may prove to be a simple and economical fix.

If the aforementioned plan does not succeed and there is still a significant leak with the new O-rings, back-up O-rings may be required. Back-up O-rings are used to help seal when the primary O-ring fails. The current design incorporates two back-up O-rings, but the material and size may have to be altered. If neither of these options work, as a last resort, the end-cap with the worst sealing issues could be welded-shut. This is not an ideal option though since once it is welded, the end-cap can never be removed. Thus if a threaded part should ever gall up and get stuck, the entire end-cap would have to be cut off and the main body re-machined in addition to a new end-cap.

REFERENCES

- ¹Sutton, G., and Biblarz, O. *Rocket Propulsion Elements*, 7th ed., John Wiley & Sons, New York, 2001.
- ²Davenas, A. "Development of Modern Solid Propellants," *Journal of Propulsion and Power* Vol. 19, No. 6, 2003, pp. 1108-1128.
- ³Allen, T., Demko, A., Johnson, M., Sammet, T., Petersen, E., Reid, D., Draper, R., and Seal, S. "Laboratory-Scale Burning of Composite Solid Propellant for Studying Novel Nanoparticle Synthesis Methods," *51st AIAA Aerospace Sciences Meeting*, Grapevine, TX, 2013.
- ⁴Stephens, M., Rodolphe, C., Steven, W., Thomas, S., Eric, P., and Christopher, S. "Performance of AP-Based Composite Propellant Containing Nanoscale Aluminum," *41st AIAA/ASME/SAE/ASEE Joint Propulsion Conference & Exhibit*, Tucson, AZ, 2005.
- ⁵Kubota, N. "Combustion of Composite Propellants," *Propellants and Explosives*. Wiley-VCH Verlag GmbH & Co. KGaA, 2007, pp. 181-233.
- ⁶Crawford, B. L., Jr., Huggett, C., Farrington, D., and Wilfong, R. E., "Direct Determination of Burning Rates of Propellant Powders," *Analytical Chemistry*, Vol. 19, No. 9, 1947, pp. 630-633.
- ⁷Boggs, T. L., Zurn, D. E., Cordes, H. F., and Covino, J., "Combustion of Ammonium Perchlorate and Various Inorganic Additives," *Journal of Propulsion and Power*, Vol. 4, No. 1, 1988, pp. 27-40.
- ⁸Chakravarthy, S. R., Price, E. W., Sigman, R. K., and Seitzman, J. M., "Plateau Burning Behavior of Ammonium Perchlorate Sandwiches and Propellants at Elevated Pressures," *Journal of Propulsion and Power*, Vol. 19, No. 1, 2003, pp. 56-65.
- ⁹Freeman, J. M., Price, E. W., Chakravarthy, S. R., and Sigman, R.K., "Contribution of Monomodal AP/HC Propellants to Bimodal Plateau-Burning Propellants," *34rd AIAA/ASME/SAE/ASEE Joint Propulsion Conference & Exhibit*, Cleveland, OH, 1998.
- ¹⁰Sippel, T. R., "Characterization of Nanoscale Aluminum and Ice Solid Propellants," MS Thesis, *Mechanical Engineering Dept.*, Purdue University, West Lafayette, Indiana, 2009.
- ¹¹Hasegawa, H., Tokudone, S., Hanzawa, M., and Kohno, M., "Erosive Burning of Aluminized Composite Propellants," *39th AIAA/ASME/SAE/ASEE Joint Propulsion Conference and Exhibit*, Huntsville, AL, 2003.

¹²Bozic, V. s., Blagojevic, D. D., and Anicin, B. A., "Measurement System for Determining Solid Propellant Burning Rate Using Transmission Microwave Interferometry," *Journal of Propulsion and Power*, Vol. 14, No. 4, 1998, pp. 421-428.

¹³Eisenreich, N., Kugler, H. P., and Sinn, F., "An Optical System for Measuring the Burning Rate of Solid Propellant Strands," *Propellants, Explosives, Pyrotechnics*, Vol. 12, 1987, pp. 78-80.

¹⁴Wang, J. and Sang, B., "Laser Technique for Determining Solid Propellant Burning Rate Measurement Techniques," *Fuel*, Vol. 77, No. 15, 1998, pp. 1845-1849.

¹⁵Iwama, A., Yamazaki, K., Kishi, K., Aoyagi, S., and Kuzuki, I., "Burning Rate Measurement of Solid Propellants by Means of Phototransistors," *Kogyo Kagaku Zasshi*, Vol 65., 1962, pp. 1218.

¹⁶Carro, R. V. "High Pressure Testing of Composite Solid Rocket Propellant Mixtures: Burner Facility Characterization," MS Thesis, *Mechanical Engineering Dept.*, Univ. of Central Florida, Orlando, Florida, 2007.

¹⁷Boggs, T. L., Price, E. W., and Zurn, D. E., "The Deflagration of Pure and Isomorphously Doped Ammonium Perchlorate," *Symposium (International) on Combustion*, Vol. 13, No. 1, 1971, pp. 995-1008.

¹⁸Chorpening, B. T. and Brewster, M. Q., "Flame Structure of Wide Distribution AP/HTPB Composite Solid Propellants From Emission Imaging," 34th AIAA/ASME/SAE/ASEE Joint Propulsion Conference & Exhibit, Cleveland, OH, 1998.

¹⁹Navaneethan, M., Srinivas, V., and Chakravarthy, S. R., "Coupling of Leading Edge Flames in the Combustion Zone of Composite Solid Propellants," *Combustion and Flame*, Vol. 153, 2008, pp. 574-592.

²⁰Mallery, C., Kim, E., and Thynell, S. T., "High-Pressure Strand Burner System for Propellant Flame Studies Using Absorption Spectroscopy," *Review of Scientific Instruments*, Vol. 66, No. 8, 1995, pp. 4091-4094.

²¹Demko, A. R., Thomas, J. C., Sammet, T., Petersen, E. L., Reid, D. L., and Seal, S., "Temperature Sensitivity of Composite Propellants Containing Novel Nano-Additive Catalysts," 50th AIAA/ASME/SAE/ASEE Joint Propulsion Conference & Exhibit, Cleveland, OH, 2014.

²²Boggs, T. L. and Zurn, D. E., "The Temperature Sensitivity of the Deflagration Rates of Pure and Doped Ammonium Perchlorate," *Combustion Science and Technology*, Vol. 4, No. 1, 1972, pp. 227-232.

²³Friedman, R., Nugent R. G., Rumbel, K. E., and Scurlock, A. C., "Deflagration of Ammonium Perchlorate," *Sixth Symposium (International) on Combustion*, pp 612.

²⁴Glaskova, A. P. and Bobolev, V. K., "Influence of the Initial Temperature of the Combustion of Ammonium Perchlorate," *Doklady Akademii Nauk SSSR*, Vol. 185, pp 346.

²⁵Maksimov, E. I., Grigor'ev, Y. M., and Merzhanov, A. G., "On the Principles and Mechanism of the Combustion of Ammonium Perchlorate," *Seriya Khimicheskaya*, No. 3, 1966, pp 422.

²⁶Shannon, L. S., "Effects of Particle Size and Initial Temperature on the Deflagration of Ammonium Perchlorate Strands," Ph. D. Thesis, Univ. of California, Berkeley, California, 1963.

²⁷Watt, D. M., Jr. and Petersen, E. E., "The Deflagration of Single Crystals of Ammonium Perchlorate," *Combustion and Flame*, Vol. 14, pp 297.

²⁸ASME Boiler and Pressure Vessel Code, Section VIII, Division I, 2007.

²⁹Carro, R., Arvanetes, J., Powell, A., Stephens, M., and Smith, C., "High-Pressure Testing of Composite Solid Propellant Mixtures: Burner Facility Characterization," *41st AIAA/ASME/SAE/ASEE Joint Propulsion Conference & Exhibit*, Tucson, AZ, 2005.

³⁰Stephens, M., Sammet, T., Carro, R., LePage, A., and Petersen, E. "Comparison of Hand and Mechanically Mixed Ap/Htpb Solid Composite Propellants," *43rd AIAA/ASME/SAE/ASEE Joint Propulsion Conference & Exhibit*. Cincinnati, OH., 2007.

APPENDIX A: MECHANICAL PROPERTIES OF 17-4 PH STAINLESS STEEL

Stainless Steel
AL 17-4™ Alloy

Technical Data BLUE SHEET

MECHANICAL PROPERTIES

	Condition A	Condition H 900	Condition H 1075	Condition H 1150
Modulus of Elasticity 10 ⁶ psi (GPa)	28.5 (196)	28.5 (196)	28.5 (196)	28.5 (196)
Modulus of Rigidity 10 ⁶ psi (GPa)	11.2 (77.2)	11.2 (77.2)	11.2 (77.2)	11.2 (77.2)

Room temperature tensile properties can vary substantially with heat treatment in the 900°F (482°C) to 1150°F (621°C) range. Values shown below are typical room temperature properties which could be expected for

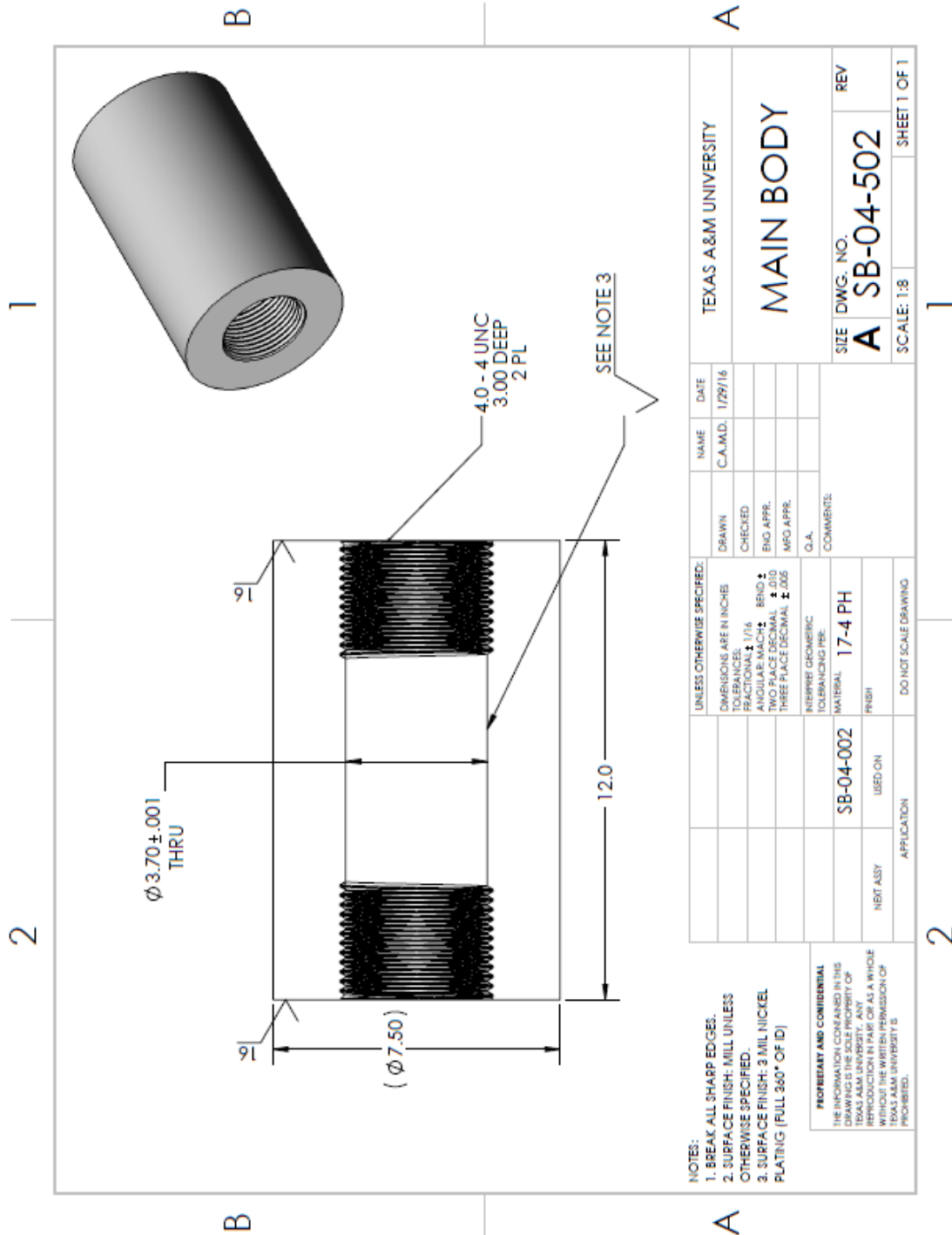
	Condition A	Condition H 900	Condition H 1075	Condition H 1150
0.2% Offset Yield Strength psi (MPa)	110,000 760	180,000 1,240	135,000 930	125,000 860
Ultimate Tensile Strength psi (MPa)	150,000 1,030	195,000 1,340	155,000 1,070	145,000 1,000
Elongation (percentage in 2")	8	10	10	10
Hardness Rockwell C scale	33	43	31	28

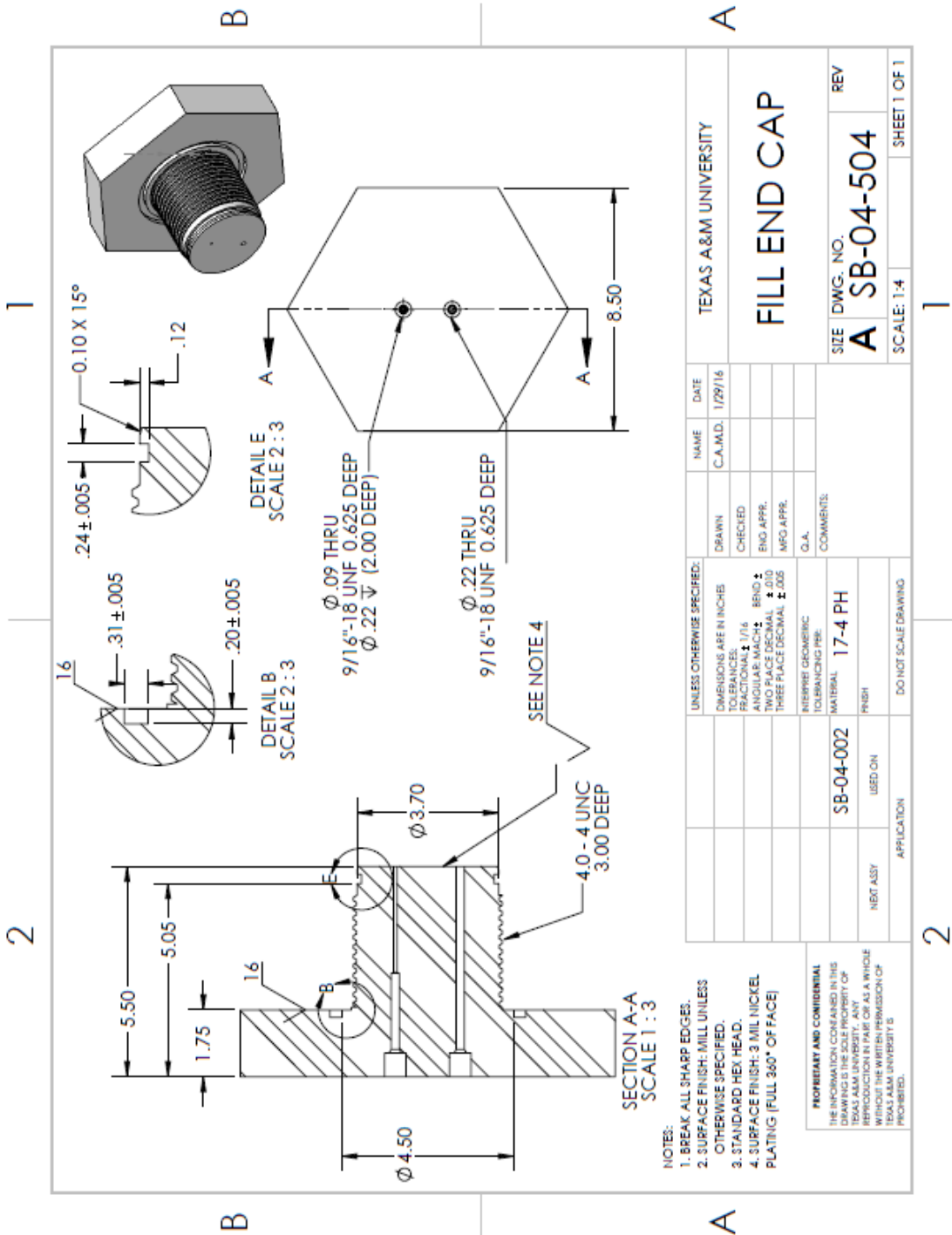
SUMMARY OF HEAT TREATING AL 17-4™ ALLOY				
Minimum Properties Specified in Aerospace Material Specification (AMS) 5604				
Heat Treat to Produce Martensitic Structure	Precipitation Heat Treatment to Produce Desired Strength			
	Precipitation Hardening Heat Treatment	Yield Strength psi (MPa)	Tensile Strength psi (MPa)	Hardness Rc
Solution Heat Treatment at 1950 °F (1066 °C)	900 °F (482 °C) 60 minutes Condition H 900	170,000 (1170)	190,000 (1310)	40 to 47
	925 °F (496 °C) 4 Hours Condition H 925	155,000 (1070)	170,000 (1170)	38 to 45
	1025 °F (552 °C) 4 Hours Condition H 1025	145,000 (1000)	155,000 (1070)	35 to 42
	1075 °F (579 °C) 4 Hours Condition H 1075	125,000 (860)	145,000 (1000)	33 to 39
	1100 °F (593 °C) 4 Hours Condition H 1100	115,000 (790)	140,000 (965)	32 to 38
	1150 °F (621 °C) 4 Hours Condition H 1150	105,000 (725)	135,000 (930)	28 to 37
Condition A (This is the condition furnished by Allegheny Ludlum)	1400 °F (760 °C) 2 Hours + 1150 °F 4 Hours Condition H 1150-M from SA 693	75,000 (515)	115,000 (790)	26 to 36

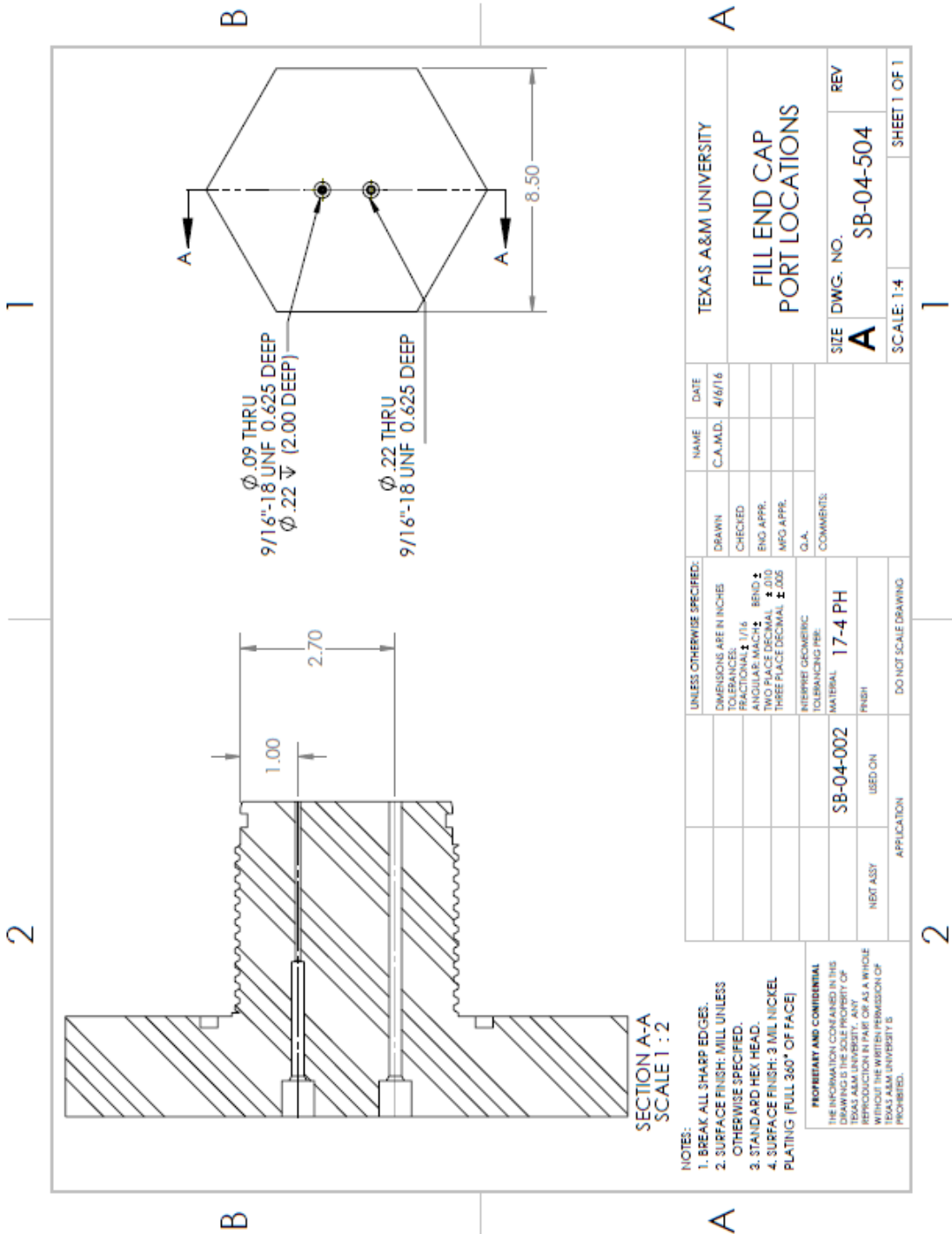
Data are typical and should not be construed as maximum or minimum values for specification or for final design. Data on any particular piece of material may vary from those shown herein.

3

APPENDIX B: STRAND BURNER IV DRAWINGS





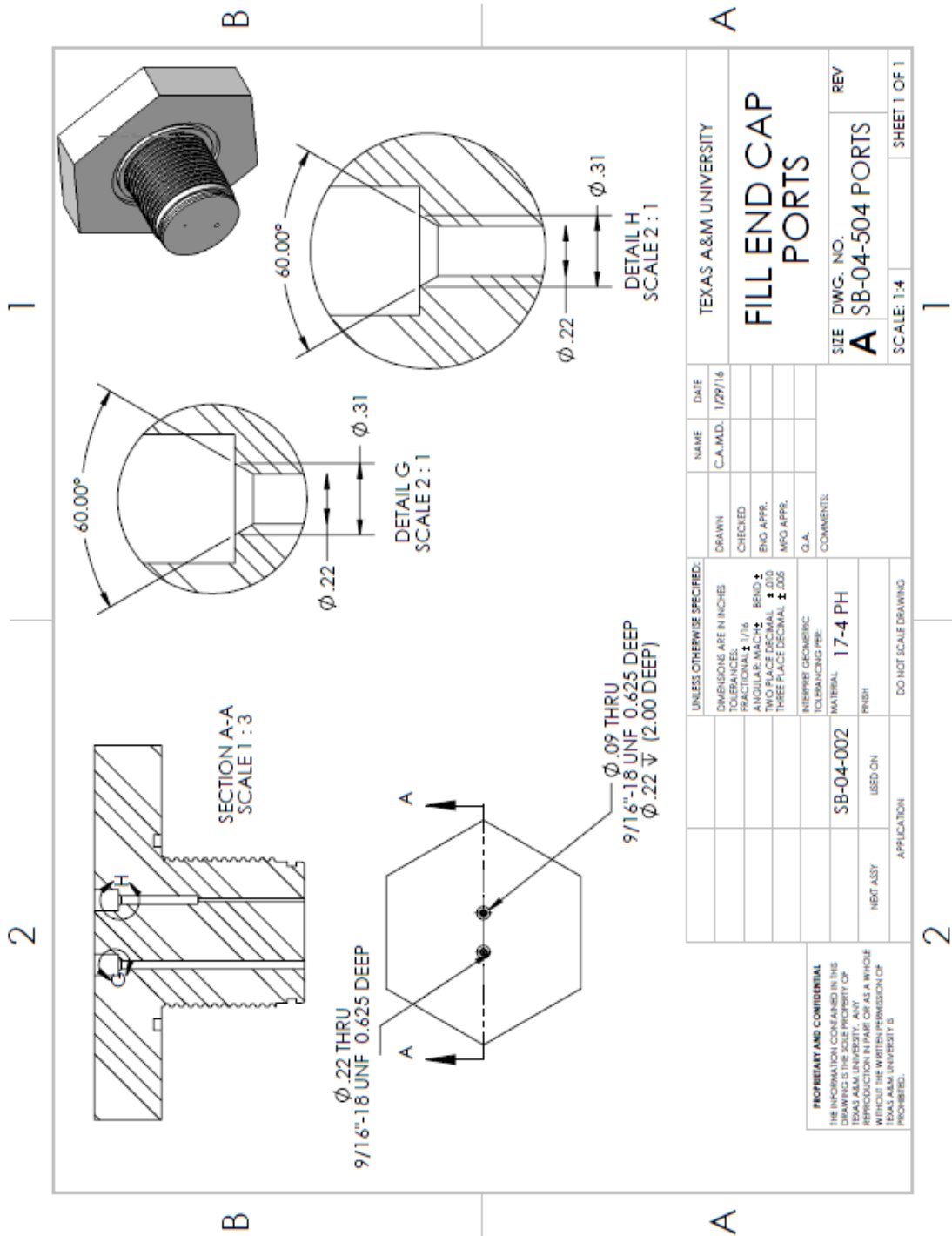


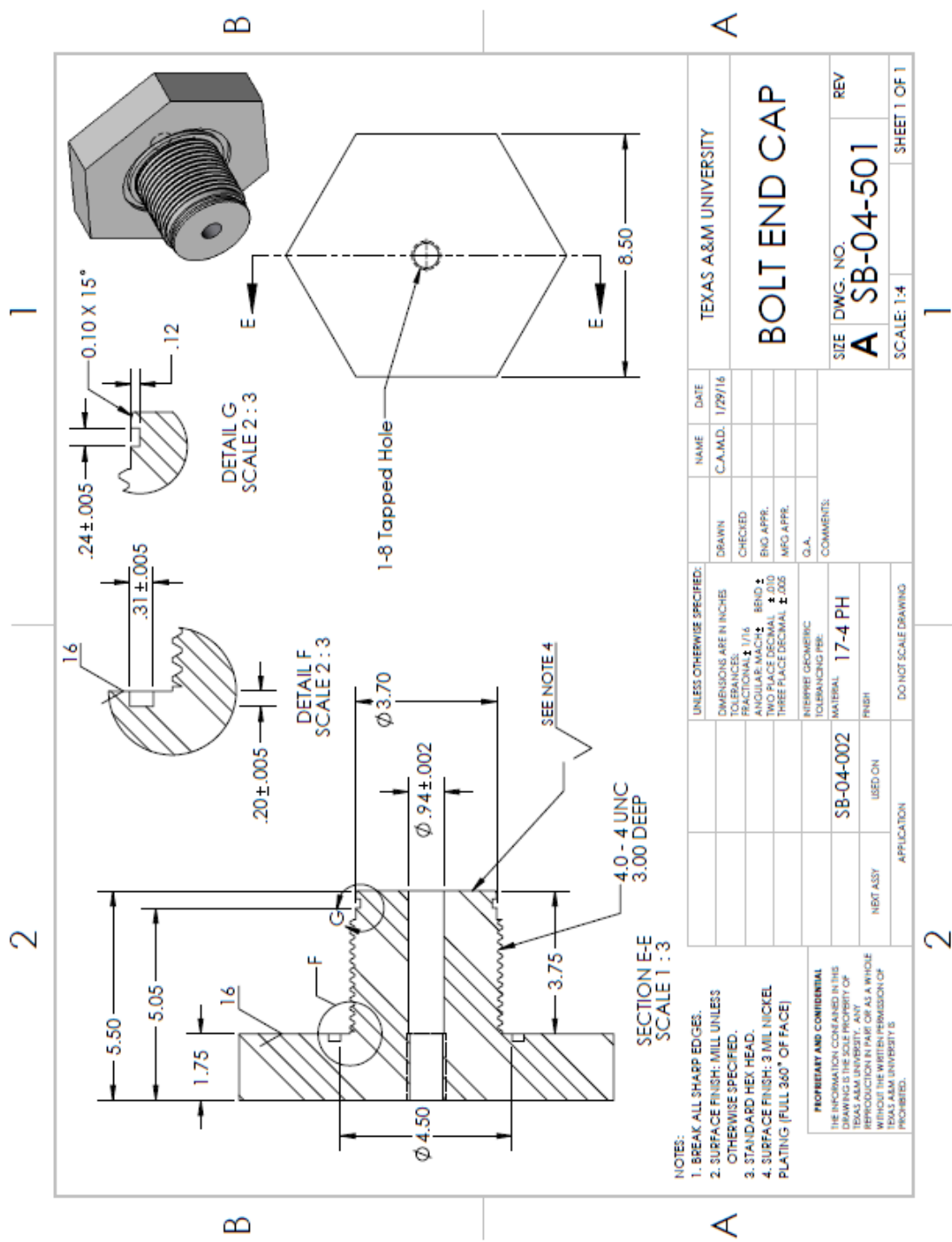
NOTES:

1. BREAK ALL SHARP EDGES.
2. SURFACE FINISH: MILL UNLESS OTHERWISE SPECIFIED.
3. STANDARD HEX HEAD.
4. SURFACE FINISH: 3 MIL NICKEL PLATING (FULL 360° OF FACE)

PROPRIETARY AND CONFIDENTIAL
THE INFORMATION CONTAINED IN THIS DRAWING IS THE SOLE PROPERTY OF TEXAS A&M UNIVERSITY. ANY REPRODUCTION IN PART OR AS A WHOLE WITHOUT THE WRITTEN PERMISSION OF TEXAS A&M UNIVERSITY IS PROHIBITED.

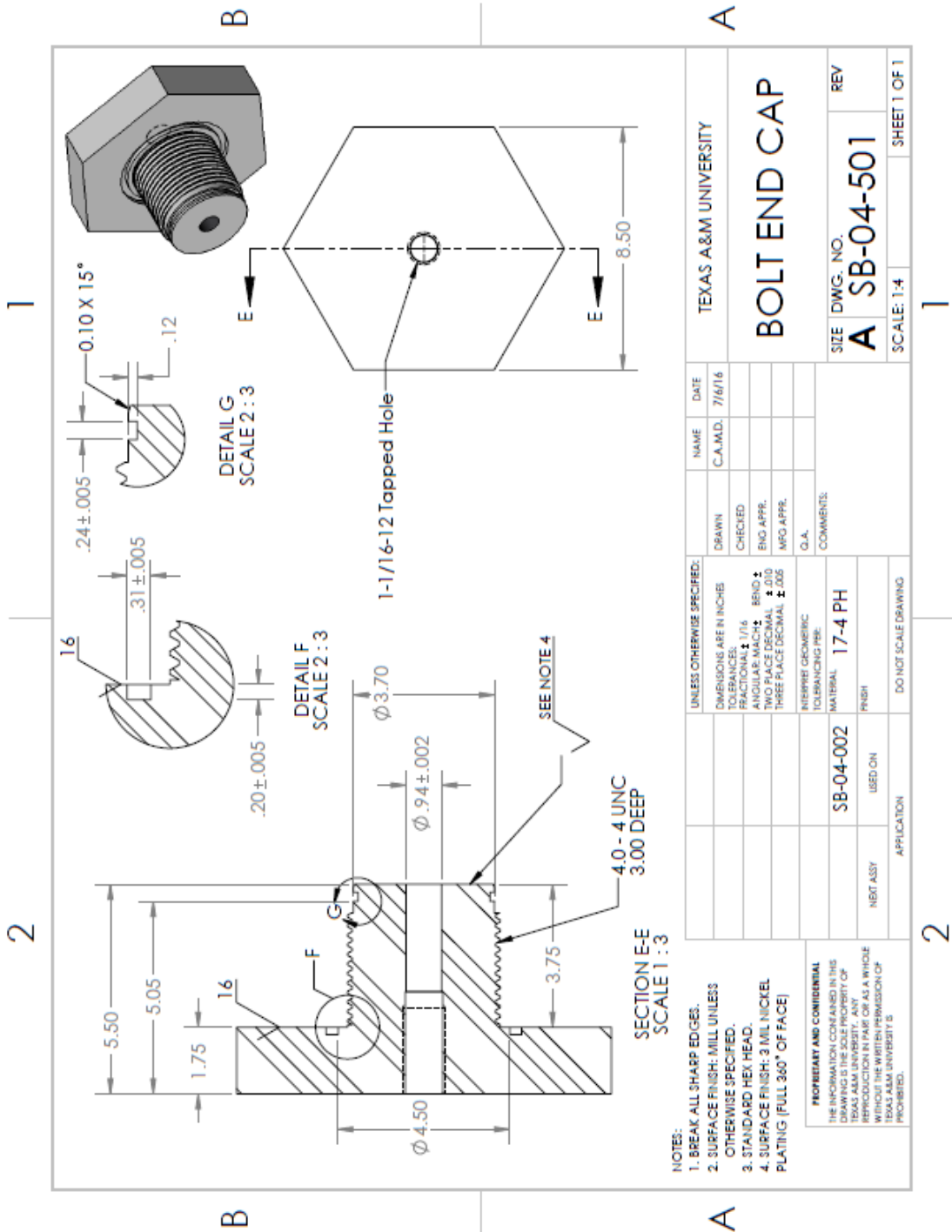
UNLESS OTHERWISE SPECIFIED:		NAME	DATE
DIMENSIONS ARE IN INCHES		C.A.M.D.	4/6/16
TOLERANCES:		DRAWN	
FRACTIONAL: $\pm 1/16$		CHECKED	
ANGULAR: MACH: $\pm 1^\circ$		END APPR.	
TWO PLACE DECIMAL: $\pm .010$		MFG APPR.	
THREE PLACE DECIMAL: $\pm .005$		G.A.	
INTERFER: CHROMIUM: TOLERANCING PER:		COMMENTS:	
MATERIAL: SB-04-002			
FINISH: 17-4 PH			
NEXT ASSY: USED ON			
APPLICATION: DO NOT SCALE DRAWING			





UNLESS OTHERWISE SPECIFIED:		NAME	DATE
DIMENSIONS ARE IN INCHES		C.A.M.D.	1/29/16
TOLERANCES:		DRAWN	
FRACTIONAL: 1/16		CHECKED	
ANGULAR: MAXIMUM ± .010		ENG APPR.	
TWO PLACE DECIMAL ± .005		WFO APPR.	
THREE PLACE DECIMAL ± .002		Q.A.	
INTERPRET GEOMETRIC TOLERANCING PER:		COMMENTS:	
MATERIAL		17-4 PH	
SB-04-002		USED ON	
NEXT ASSY		APPLICATION	
DO NOT SCALE DRAWING			

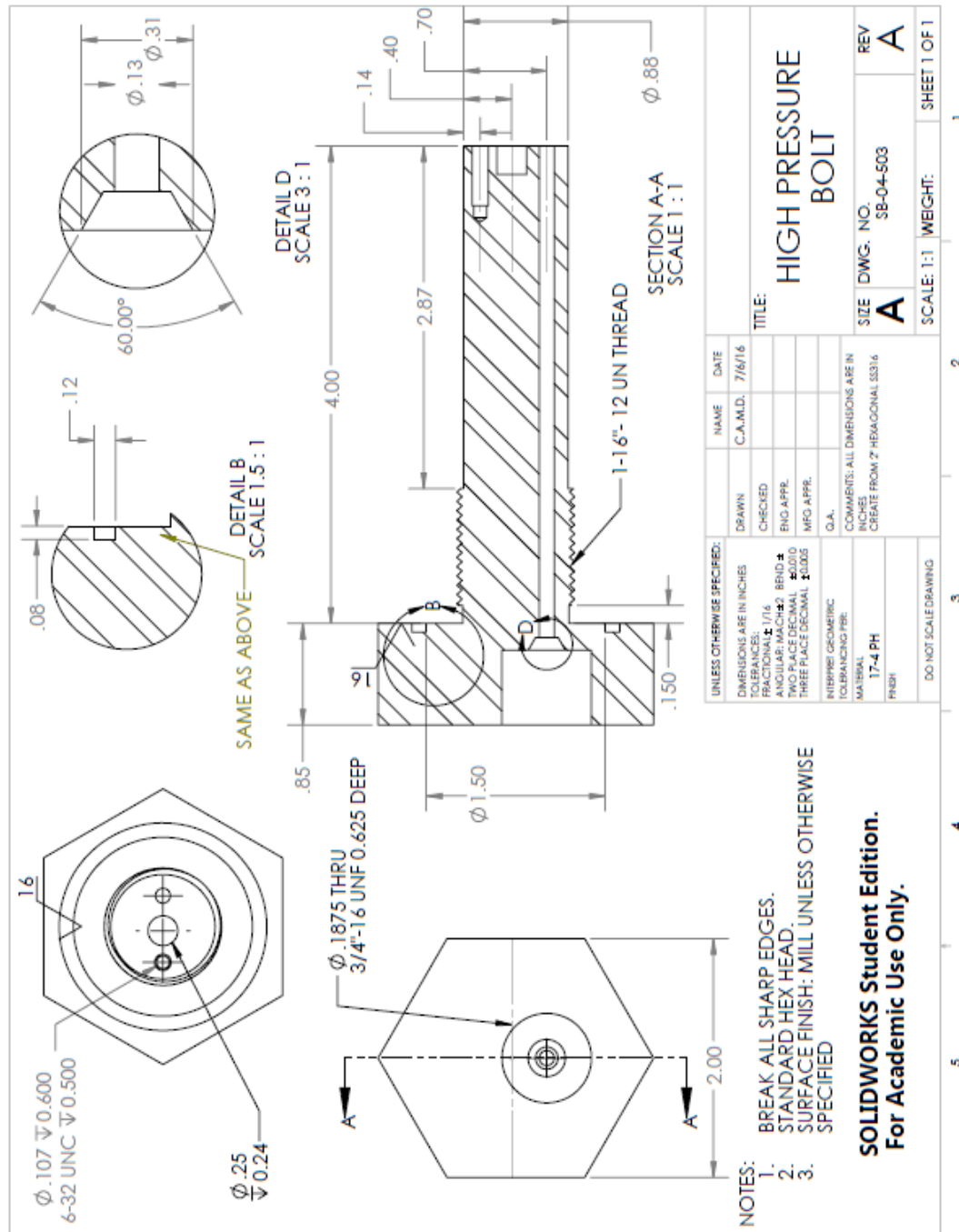
TEXAS A&M UNIVERSITY	
BOLT END CAP	
SIZE	DWG. NO.
A	SB-04-501
SCALE: 1:4	SHEET 1 OF 1

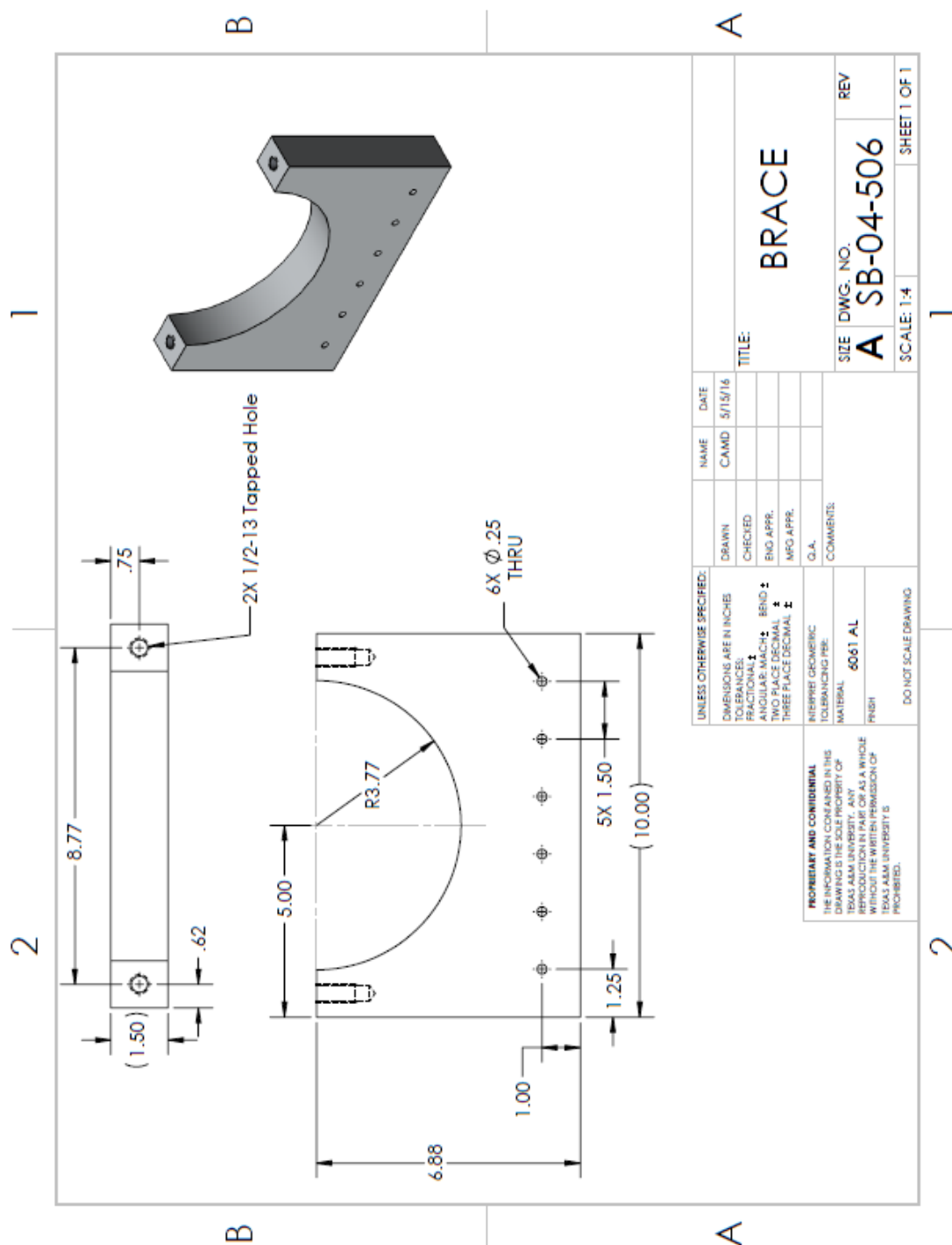


- NOTES:**
1. BREAK ALL SHARP EDGES.
 2. SURFACE FINISH: MILL UNLESS OTHERWISE SPECIFIED.
 3. STANDARD HEX HEAD.
 4. SURFACE FINISH: 3 MIL NICKEL PLATING (FULL 360° OF FACE)

PROPRIETARY AND CONFIDENTIAL
THE INFORMATION CONTAINED IN THIS DRAWING IS THE SOLE PROPERTY OF TEXAS A&M UNIVERSITY. ANY REPRODUCTION IN PART OR AS A WHOLE WITHOUT THE WRITTEN PERMISSION OF TEXAS A&M UNIVERSITY IS PROHIBITED.

		UNLESS OTHERWISE SPECIFIED:			NAME	DATE	TEXAS A&M UNIVERSITY	
		DIMENSIONS ARE IN INCHES TOLERANCES:		DRAWN	C.A.M.D.	7/6/16		
		FRACTIONAL: $\pm 1/16$		CHECKED				
		ANGULAR: MACH \pm .010		ENG APPR.				
		TWO PLACE DECIMAL \pm .010		MFG APPR.				
		THREE PLACE DECIMAL \pm .005		G.A.				
		INTERPRET GEOMETRIC TOLERANCING PRE:		COMMENTS:				SIZE DWG. NO. REV A SB-04-501
		MATERIAL		17-4 PH				
		FINISH						
		USED ON						
		NEXT ASSY						
APPLICATION				SCALE: 1:4				SHEET 1 OF 1





APPENDIX C: FACILITY HARDWARE



ENGINEERS AND MANUFACTURERS OF ULTRA-LOW FREEZERS

SO-LOW CHEST STYLE FREEZER TO -85°C

MODEL C85-3

3 Cubic Ft. (83 liters) Chest – Temperature Range: -40°C to -85°C

Top Opening

Specifications:

* Capacity	3 cubic ft. / 83 liters
* Temperature Range	-40°C to -85°C
* Dimensions	
* Exterior W x D x H	34" x 27" x 47" 86 x 69 x 119 (cm)
* Interior W x D x H	24" x 12" x 18" 61 x 31 x 46 (cm)

Voltage:

115 volts, 60 hertz, 1 phase
208 volts, 60 hertz, 1 phase
230 volts, 60 hertz, 1 phase
220 volts, 50 hertz, 1 phase
15 AMP dedicated circuit required.
ETL electrical approval.

TEMPERATURE CONTROL

Microprocessor control displays set point and chamber temperature.

ALARM SYSTEM WITH RELAY

The battery operated alarm system will emit an audible and visual signal when there is a mechanical or electrical failure. The alarm has an over and under temperature setting, alarm silencing switch, and battery test switch. Also provided is a relay for remote alarm hook-up.

REFRIGERATION SYSTEM

A So-Low cascade system with two hermetic compressors. CFC & HCFC free refrigerants

CONSTRUCTION

Chamber is 14-ga. Zinc coated galvanized steel. Exterior is 16-ga. steel. Power coated cool gray.

TECHNICAL SUPPORT

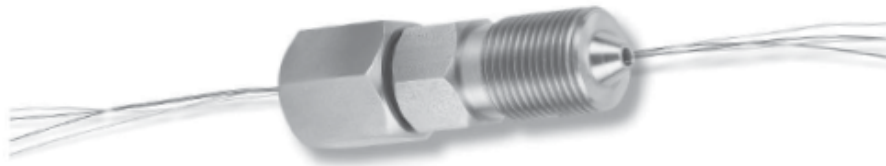
Supplied by Nation-Wide-Network of service companies.

Specifications subject to change without notice



5001D

HPPL SERIES ■ HIGH PRESSURE SEALING ASSEMBLIES UP TO 30,000 PSIG



High Pressure Sealing Insulated Wire Glands (HPPL)

Conax Technologies manufactures high pressure seals (up to 30,000 psig at 68°F (20°C)) for instrument signal wires. High pressure seals are designed for installation onto the pressure vessel wall using threaded mounting configurations only. High pressure assemblies are factory torqued, so disassembly and reassembly in the field is not recommended.

These assemblies feature body and caps constructed from high strength 316SST and a proprietary sealant. HPPL assemblies are provided with Kapton-insulated 26 gauge solid copper wire or 24 gauge thermocouple wire. Standard assemblies include 24" of wire on each side. To order other wire lengths, indicate the desired lengths after the catalog number.

A 1/2" NPT thread can be added to the assembly cap to allow mounting a terminal box or other type of enclosure. Consult factory for ordering details.

For other types of high pressure applications such as electrode sealing, please consult the factory.

Specifications – High Pressure Assemblies

Catalog Number	Wire Gauge	Number of Wires	Length IN MM	Thread Size	Body IN	Cap IN	Hex Size Body MM	Cap MM	Pressure Rating PSIG BAR
HPPL14(AM3/S316B)-26-A/S316B*-CGL	26	2-7	3.00 76.2	3/4-16	1.250	1.000	31.8	25.4	30,000 2067
HPPL8(AM6/S316B)-26-A/S316B*-CGL	26	2-10	3.00 76.2	1 1/8-12	1.250	1.250	31.8	31.8	20,000 1378
HPPL14(AM3/S316B)-24-A/S316B*-CGL	24	2-6	3.00 76.2	3/4-16	1.250	1.000	31.8	25.4	20,000 1378
HPPL8(AM6/S316B)-24-A/S316B*-CGL	24	2-6	3.00 76.2	1 1/8-12	1.250	1.250	31.8	31.8	20,000 1378

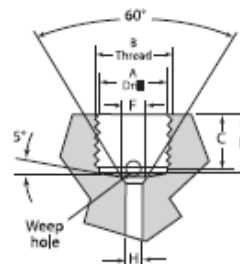
Note: HPPL 14 males with Snap-It/Autoclave Engineers part type F-375-C. HPPL 8 males with Snap-It/Autoclave Engineers part type F-562-C.

Tube Connection Dimensions – Autoclave High Pressure FC

Tube Outside	Connection Type	A	B	Dimensions Inches (mm) C D	F	H
1/4	F250C	3/16 (13.1)	9/16 -18	0.38 (9.7) 0.44 (11.1)	0.17 (4.3)	0.094 (2.4)
3/8	F375C	11/16 (17.4)	3/4 -16	0.53 (13.5) 0.62 (15.7)	0.26 (6.6)	0.125 (3.2)
9/16	F562C	1-3/16 (26.6)	1-1/8 -12	0.62 (15.7) 0.75 (19.1)	0.38 (9.7)	0.188 (4.8)
9/16	F562C40	1-3/16 (26.6)	1-1/8 -12	0.62 (15.7) 0.75 (19.1)	0.38 (9.7)	0.250 (6.4)
5/16	F312C150	3/16 (14.7)	5/8 -18	0.62 (15.7) 1.06 (26.9)	0.25 (6.4)	0.094 (2.4)

Note: All dimensions are shown for reference only and should not be considered as actual machining dimensions.
All threads are manufactured to a class 2A or 2B fit.

* Body side wire length 80" (203.2 cm) maximum. Consult factory for longer lengths.



Example: HPPL14(AM3/S316B)-26-A/(S316B)2-CGL, 30/45

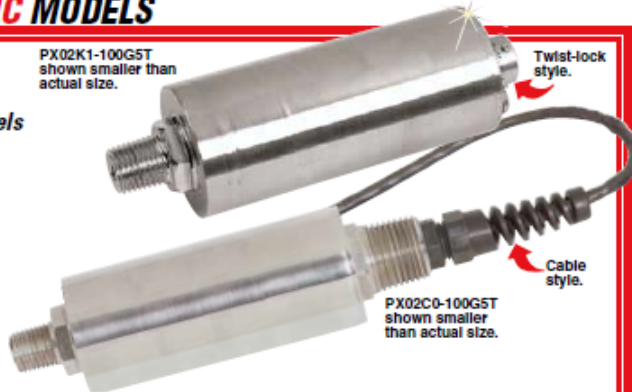
HIGH-ACCURACY AMPLIFIED VOLTAGE OUTPUT PRESSURE TRANSDUCER **STANDARD AND METRIC MODELS**

0 to 5 Vdc Output
0-2 to 0-30,000 psi-Standard Models
0-150 mbar to 0-400 bar-Metric Models

PX02/PXM02 Series



PX02K1-100GST
shown smaller than
actual size.



PX02C0-100GST
shown smaller than
actual size.

VOLTAGE OUTPUT
PRESSURE TRANSDUCERS
B

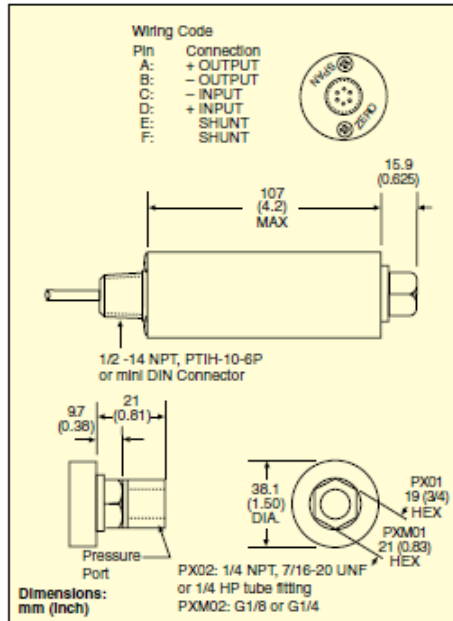
- ✓ Internal Shunt Resistor for Easy System Checks
- ✓ All Stainless Steel Construction
- ✓ Available in Gage, Absolute, Sealed Gage, psi, and Metric Ranges
- ✓ Cable, Connector Models or Mini DIN
- ✓ Optional Pressure Ports to Fit Most Industrial Applications

Proof Pressure: 150% of rated pressure
Burst Pressure: 300% of rated pressure
Wetted Parts: 17-4 PH stainless steel
Pressure Port: See custom configurations
Electrical Connection: See custom configurations
Mating Connector: (Style 1) PT06F10-6S (sold separately)
Weight: 388 g (13.7 oz)

OMEGA's PX02/PXM02 are high-accuracy, amplified voltage output, industrial pressure transducers. All stainless steel construction and a hermetically sealed case make the PX02/PXM02 suitable for harsh industrial environments. They are a true high-accuracy industrial device.

SPECIFICATIONS

Excitation: 24 to 32 Vdc
Output: 0 to 5 Vdc $\pm 10\%$ adjustable
Linearity: $\pm 0.15\%$ FSO
Hysteresis: $\pm 0.1\%$ FSO
Repeatability: $\pm 0.05\%$ FSO
Zero Balance: 0 V $\pm 10\%$ adj
Sensing Element: 4-active-arm bridge, using thick-film strain gages in a hermetically sealed chamber (except gage units)
Shunt Calibration Value: Specified on calibration sheet
Operating Temp Range: -46 to 121°C (-50 to 250°F)
Compensated Temp Range: 16 to 71°C (60 to 160°F)
Thermal Effects:
Span: 0.003% of rdg/°F
Zero: 0.003% of FSO/°F



B-124

1/8 DIN HIGH-PERFORMANCE METERS

ALARM/CONTROL CAPABILITIES

STRAIN GAGE, PROCESS VOLTAGE AND CURRENT, TEMPERATURE

DP41 Series



DP41-S strain meter shown actual size.

All Units Feature:

- ✓ 5-Year Warranty
- ✓ 6-Digit Display
- ✓ Min/Max Storage
- ✓ 4 Isolated Open-Collector Outputs
- ✓ NEMA 4 (IP65) Front Panel
- ✓ 12 Readings per Second
- ✓ Alarm/Control Capabilities
- ✓ Smart Filtering Detects the Difference Between a Spike or Process Change (Patent Applied for)
- ✓ Peak and Valley Detection
- ✓ Digital Tare
- ✓ Easy Front-Panel Programming
- ✓ Optional BCD Output
- ✓ Optional Analog Output
- ✓ Optional RS232/RS485 Communications
- ✓ Optional Mechanical Relays
- Thermocouple Input:**
 - ✓ 0.01° Resolution
 - ✓ 0.2°C Accuracy
 - ✓ 9 Thermocouple Types
 - ✓ °C/°F/K Units
- Uses Complete NIST Calibration Tables**
- RTD Input:**
 - ✓ 0.01° Resolution
 - ✓ 0.2°C Accuracy
 - ✓ 2-, 3-, or 4-Wire
 - ✓ 385 and 392 Pt Curves

Voltage/Current Inputs:

- ✓ ±0.005% Rdg Accuracy
- ✓ 10 User-Selectable Voltage or 4 to 20/0 to 20 mA Input Ranges
- ✓ Fully Scalable Display Up to 500,000 Counts
- ✓ 1.5 to 11 Vdc or 24 Vdc Sensor Excitation
- ✓ Adjustable Decimal Point

The OMEGA® DP41 Series of digital panel meter/controllers has set the world standard for accuracy and quality in industrial instrumentation. These meters can measure a broad spectrum of DC voltage and current ranges as well as inputs from 9 thermocouple types and from most RTDs, pressure transducers, load cells, strain gages, and potentiometers. Models include the DP41-W, a legal-for-trade, NTEP-certified strain meter with enhanced features, and the DP41-U, which covers all the input types.

Standard features include 6-digit display; 5 front-panel pushbutton keys; 4 open-collector outputs; and alarm/control, BCD, and analog outputs. Configurable analog output ranges are 0 to 20 mA, 4 to 20 mA, 0 to 5 Vdc, and 0 to 10 Vdc.

On-board excitation allows these meters to power virtually any sensor or transmitter, and 4 setpoints give the user numerous control/alarm possibilities. Setpoint configurations include active above or below; latching or non-latching; and high deviation, low deviation, or band deviation.

With the RS232/485 serial communications option, the user can set the display parameters and read the current, max, and min values remotely. The DP40-R board option provides dual 7 A mechanical relays, activated by the selected setpoint.

MONOGRAM® SERIES

The DP41 displays feature 14-segment LED characters, which greatly improves alphanumeric representations. The 7-segment LED characters found on most instruments are adequate for presenting numbers, but not letters. Words are easier to read with the 14-segment LED characters on the DP41, which, in turn, simplifies operating and programming.

RESET2

14-segment LED

RESET2

7-segment LED



Red LED display standard. Also available with green LED at no charge.

D-29

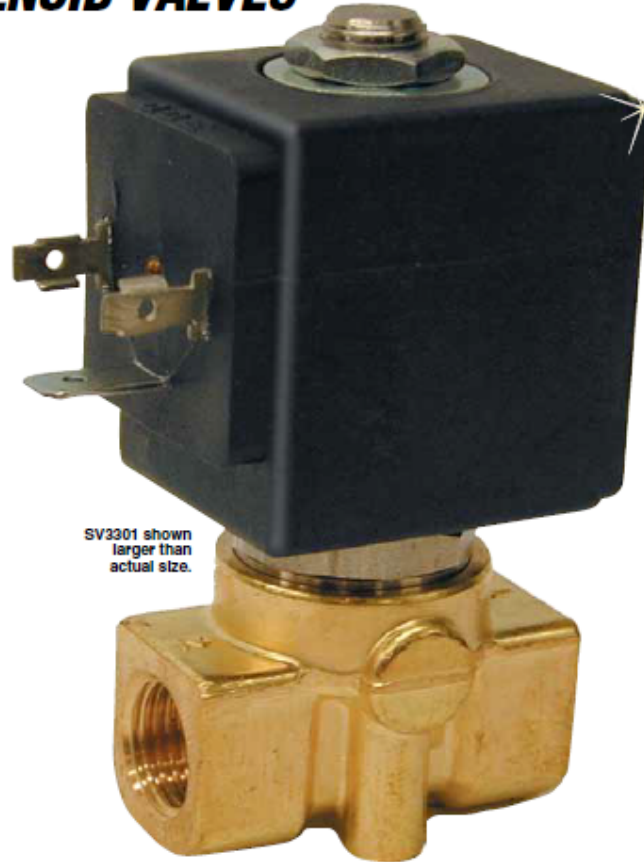
OMEGA-FLO® 2-WAY GENERAL PURPOSE SOLENOID VALVES

SV3300 Series



- ✓ Ideal for Compressed Air, Inert Gas, Water and Synthetic Oils
- ✓ Available in Normally Open or Normally Closed
- ✓ Process Temperature to 137°C (280°F)
- ✓ 8 W, AC Coils Standard, 12 or 14 W, AC or DC Coils Available

SV-3300 Series 2-way solenoid valves are direct-acting valves featuring brass, stainless steel construction and FKM seal material. The temperature range from -10 to 137°C (14 to 280°F) is ideal for neutral media such as compressed air, inert gases, water, and synthetic oils. A strain-relief connector is supplied with each unit. A ½" conduit plug is also available.



SV3301 shown larger than actual size.

SPECIFICATIONS

Mounting Position: Any (preferably with solenoid system upright)

Maximum Process Temperature: 137°C (280°F) due to FKM O-ring

Maximum Ambient Temperature:

Coil Dependent (See ratings on coils)

Voltage Tolerance: ±10%

Opening Time (msec):

AC: 10 to 20

DC: 20 to 80 depending on orifice and pressure

Closing Time (msec):

AC and DC: 20 to 30 approximately

Cycling Rate: Approx. 1000 cpm

Duty Cycle: Continuous (100%)

Coil Molding Material:

Black Polyester (Class F):

SV8COIL-115AC

SV8COIL-24DC/60HZ

SVCOIL-24AC/50 to 60HZ

SV8COIL-220AC

Black Polyamide (Class F):

SV8COIL-12DC, SV8COIL-24DC,

all 12 Watt coils

Black Polyphenylsulfide (Class H):

SV8COIL-115/60HZ

Black Epoxy Resin (Class H):

All 14 Watt coils

Materials of Construction

Body	Brass
Armature Tube	Stainless Steel 300
Fixed Core	Stainless Steel 400
Plunger	Stainless Steel 400
Spring	Stainless Steel 300
Shading Ring	Copper
Orifice ≤ ¼"	Stainless Steel 300
Orifice > ¼"	Brass
Sealing Material	FKM

Coil Specifications

Coil	Inrush VA	Holding VA
8 W	25	14
12 W	36	23
14 W	43	27

J-13



High Pressure Equipment

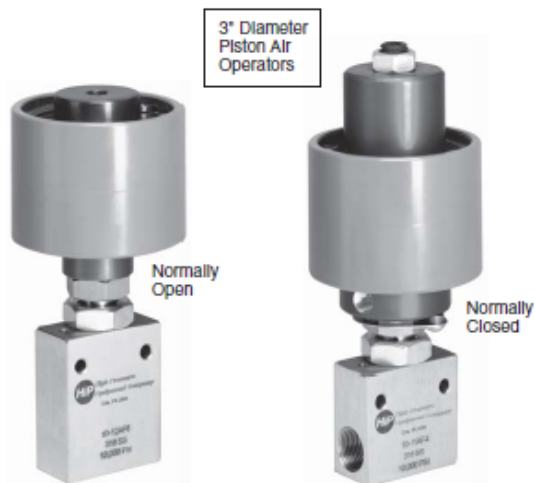
Mini-Hippo Piston Air Operators for Remote Operation To 6,000 psi

Mini-Hippo Air Operators are available for both normally open service (spring to open/air to close) and for normally closed service (air to open/spring to close). These piston air operators provide remote automatic on/off operation of valves and can be controlled by means of an air regulator, an electrical solenoid, or a manual low pressure valve in the user's air supply line. Air inlet is $\frac{1}{4}$ " NPT. Air pressure requirement ranges from 50 to 90 psi.

The Mini-Hippo air operators may be supplied with the valves and operating pressures shown in table.

To order simply specify catalog number of valve and type operation required.

EXAMPLES: Mini-Hippo 30-11HF4 (normally closed)
Mini-Hippo 10-12AF6 (normally open)
Mini-Hippo 10-15AF4 (normally open/
normally closed)



Normally Open (Spring To Open / Air To Close)

Valve Series	Maximum Operating Pressure	Approximate Air Pressure to Seat Valve
10-11AF2	6,000 psi	55 psi
10-11AF4	6,000 psi	55 psi
10-11AF6	6,000 psi	55 psi
30-11HF4	6,000 psi	55 psi
30-11HF6	6,000 psi	55 psi
30-11HF9	6,000 psi	55 psi

Normally Closed (Air To Open / Spring To Close)

Valve Series	Maximum Operating Pressure	Minimum Adjusting Screw Torque	Approximate Air Pressure to Unseat Valve	Approximate Air Pressure to Fully Open Valve
10-11AF4	6,000 psi	15 in. lb.	50 psi	90 psi
10-11AF6	6,000 psi	15 in. lb.	50 psi	90 psi
30-11HF4	6,000 psi	15 in. lb.	50 psi	90 psi
30-11HF6	6,000 psi	15 in. lb.	50 psi	90 psi
30-11HF9	6,000 psi	15 in. lb.	50 psi	90 psi

** Standard Valve Patterns (reference Page 1.4)

OPTIONS: **Stems & Seats** . . . Carbide (for cyclic service)
Stellite (for cyclic service)
17-4 (for cyclic service)

Valve Bodies . . . Hastelloy C, Hastelloy B
Inconel 600, Inconel 625
Incoloy 800, Incoloy 825
Titanium Grade 2, Titanium 6AL4V
Nickel
Monel

Packing PolyPak

Temperature Considerations . . . Extended stuffing box for temperatures from -423°F to 1,200°F (medium and high pressure connections only)

Air Operated Valves

Hipco Diaphragm Air Operators for Remote Operation To 60,000 psi

Hipco Air Operators are available for both normally open service (spring to open/air to close) and for normally closed service (air to open/spring to close). These diaphragm air operators provide remote automatic on/off operation of valves and can be controlled by means of an air regulator, an electrical solenoid, or a manual low pressure valve in the user's air supply line. Air inlet is $\frac{1}{4}$ " NPT.

The Hipco air operators may be supplied with the valves and operating pressures shown in table.

To order simply specify catalog number of valve and type operation required.

EXAMPLES: Hipco 30-11HF4 (normally closed)
Hipco 10-12NFB (normally open)
Hipco 10-15AF4 (normally open/normally closed)

OPTIONS: Stems & Seats . . . Carbide (for cyclic service)
Stellite (for cyclic service)
17-4 (for cyclic service)

Valve Bodies . . . Hastelloy C, Hastelloy B
Inconel 600, Inconel 625
Incoloy 800, Incoloy 825
Titanium Grade 2,
Titanium 6AL4V
Nickel
Monel

Packing PolyPak

Temperature

Considerations . . . Extended stuffing box for temperatures from -423°F to 1,200°F (medium and high pressure connections only)



Normally Open (Spring To Open / Air To Close)

Valve Series	Maximum Operating Pressure	Approximate Air Pressure to Seat Valve
10- **AF4	10,000 psi	35 psi
10- **AF6	10,000 psi	35 psi
10- **NFA	10,000 psi	35 psi
10- **NFB	10,000 psi	35 psi
10- **NFC	10,000 psi	35 psi
15F- **NFA	15,000 psi	85 psi
15F- **NFB	15,000 psi	85 psi
15F- **NFC	10,000 psi	100 psi
15F- **NFD	10,000 psi	100 psi
20- **LF4	20,000 psi	60 psi
20- **LF6	15,000 psi	85 psi
20- **LF9	10,000 psi	100 psi
30- **HF4	30,000 psi	60 psi
30- **HF6	30,000 psi	85 psi
30- **HF9	30,000 psi	85 psi
40- **HF9	30,000 psi	85 psi
60- **HF4	60,000 psi	70 psi
60- **HF6	60,000 psi	70 psi
60- **HF9	60,000 psi	70 psi

Normally Closed (Air To Open / Spring To Close)

Valve Series	Maximum Operating Pressure	Minimum Adjusting Screw Torque	Approximate Air Pressure to Unseat Valve	Approximate Air Pressure to Fully Open Valve
10- **AF4	10,000 psi	20 in. lb.	30 psi	45 psi
10- **AF6	10,000 psi	20 in. lb.	30 psi	45 psi
10- **NFA	10,000 psi	20 in. lb.	30 psi	45 psi
10- **NFB	10,000 psi	20 in. lb.	30 psi	45 psi
10- **NFC	10,000 psi	20 in. lb.	30 psi	45 psi
15F- **NFA	15,000 psi	60 in. lb.	80 psi	100 psi
15F- **NFB	15,000 psi	60 in. lb.	80 psi	100 psi
15F- **NFC	10,000 psi	75 in. lb.	95 psi	100 psi
15F- **NFD	10,000 psi	75 in. lb.	95 psi	100 psi
20- **LF4	20,000 psi	40 in. lb.	55 psi	90 psi
20- **LF6	15,000 psi	60 in. lb.	80 psi	100 psi
20- **LF9	10,000 psi	75 in. lb.	95 psi	100 psi
30- **HF4	30,000 psi	40 in. lb.	55 psi	75 psi
30- **HF6	30,000 psi	60 in. lb.	80 psi	100 psi
30- **HF9	30,000 psi	60 in. lb.	80 psi	100 psi
40- **HF9	30,000 psi	60 in. lb.	80 psi	100 psi
60- **HF4	60,000 psi	50 in. lb.	65 psi	85 psi
60- **HF6	60,000 psi	50 in. lb.	65 psi	85 psi
60- **HF9	60,000 psi	50 in. lb.	65 psi	85 psi

** Standard Valve Patterns (reference Page 1.4)

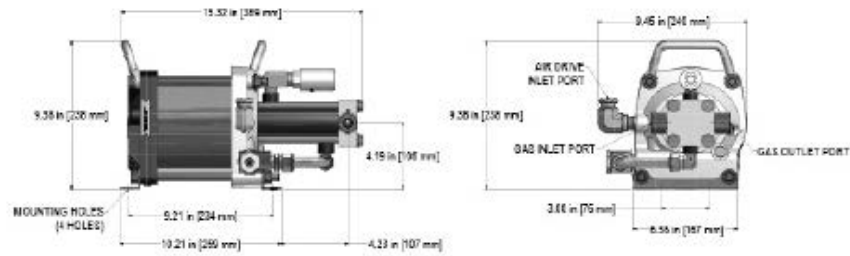
High Pressure Equipment Company

2965 W. 17th Street • Erie, PA 16505 U.S.A. • Phone: (814) 838-2028 • 1-800-289-7447 • Fax: (814) 838-6075 • Website: www.HighPressure.com

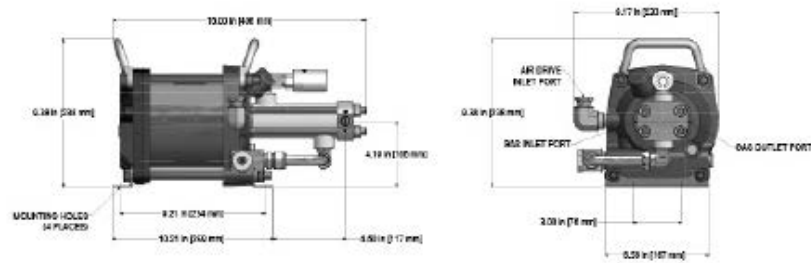
R4 2/02

7.2

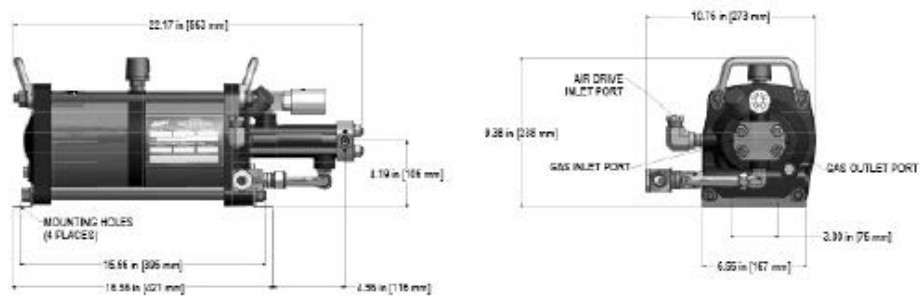
Gas Booster Model: AG-7



Gas Booster Models: AG-15, AG-30, AG-50, AG-75



Gas Booster Models: AG-62, AG-102, AG-152



Model Selection Chart

LEGEND: P_s = Gas Supply Pressure, P_a = Drive Pressure, P_o = Outlet Pressure

	Model Number	Maximum Rated Gas Supply		Min. Gas Supply Pressure		Maximum Rated Gas Outlet						Static Outlet Stall Pressure Formula	Piston Displacement Per Cycle		Gas Inlet/Outlet Connections	Weight
						Inert Gas		Oxygen		Hydrogen						
		PSIG	BAR	PSIG	BAR	PSIG	BAR	PSIG	BAR	PSIG	BAR		Cu. In.	ML		LB (KG)
Single Acting Single Stage Model AG	4AG-25	4500	310	25	1.7	4500	310	4500	310	N/A	N/A	25 Pa	1.23	20.2	3/8" SAE Both Ports	12 (6)
	AG-4	1250	86	ATM	ATM	1250	86	1250	86	N/A	N/A	4 Pa	10	163.9	3/8" NPT Both Ports	25 (11)
	AG-7	1060	72	25	1.7	1060	72	1060	72	N/A	N/A	7 Pa	13.2	210.3	3/8" NPT Both Ports	30 (14)
	AG-15	2250	155	50	3.5	2250	155	2250	155	N/A	N/A	15 Pa	6.2	101.8	Interchangeable 3-3/8" SAE or 1/4" NPT (Both Ports) Both Ports	27 (12)
	AG-30	4500	310	100	7	4500	310	4500	310	4500	310	30 Pa	3.1	50.8	Interchangeable 3-3/8" SAE or 1/4" NPT (Both Ports) Both Ports	27 (12)
	AG-50	7500	517	100	7	7500	517	5000	345	N/A	N/A	50 Pa	1.96	32.1	Interchangeable 3-3/8" SAE or 1/4" NPT (Both Ports) Both Ports	27 (12)
	AG-62	9000	620	200	14	9000	620	5000	345	9000	620	60 Pa	3.1	50.8	Interchangeable 3-3/8" SAE or 1/4" NPT (Both Ports) Both Ports	35 (16)
	AG-75	11250	775	250	17	11250	775	5000	345	11250	775	75 Pa	1.2	19.6	Interchangeable 3-3/8" SAE or 1/4" NPT (Both Ports) Both Ports	27 (12)
	AG-102	7500	517	100	7	15000	1034	5000	345	N/A	N/A	100 Pa	1.96	32.1	Interchangeable 3-3/8" SAE or 1/4" NPT (Both Ports) Both Ports	35 (16)
	AG-152	20000	1380	250	17	20000	1380	5000	345	15000	1034	150 Pa	1.2	19.6	Interchangeable 3-3/8" SAE or 1/4" NPT (Both Ports) Both Ports	27 (12)
	AG-233	22500	1551	250	17	22500	1551	N/A	N/A	N/A	N/A	225 Pa	1.2	19.6	Interchangeable 3-3/8" SAE or 1/4" NPT (Both Ports) Both Ports	40 (18)
	AG-303	39000	2690	500	34	39000	2690	N/A	N/A	N/A	N/A	300 Pa	0.89	14.6	1/4" NPT (Both Ports) Both Ports	44 (20)
Double Acting Single Stage Model AGD	AGD-1.5	300	21	ATM	ATM	300	21	300	21	N/A	N/A	1.5 Pa+Pa	60	963.2	Inlet Port 3/4" NPT Outlet Port 1/2" NPT	44 (20)
	AGD-4	1250	86	ATM	ATM	1250	86	1250	86	N/A	N/A	4 Pa+Pa	16.3	310.3	3/8" NPT Both Ports	31 (14)
	AGD-7	2500	172	25	1.7	2500	172	2500	172	2500	172	7 Pa+Pa	26.4	432.8	Inlet Port 3/8" NPT Outlet Port 3/8" NPT 2 ea. inlet & outlet	35 (16)
	AGD-14	5000	345	25	1.7	5000	345	5000	345	N/A	N/A	14 Pa+Pa	20.4	432.8	Inlet Port: 3/8" NPT Outlet: 3/8" NPT	49 (22)
	AGD-15	5000	345	50	3.5	5000	345	5000	345	4000	270	15 Pa+Pa	12.4	203.2	Interchangeable 3-3/8" SAE or 1/4" NPT both Ports. 2 ea. Inlet & outlet	35 (16)
	AGD-30	9000	620	100	7	9000	620	5000	345	9000	620	30 Pa+Pa	6.2	101.8	Interchangeable 3-3/8" SAE or 1/4" NPT both Ports. 2 ea. Inlet & outlet	38 (17)
	AGD-32	5000	345	50	3.5	5000	345	5000	345	4000	270	30 Pa+Pa	12.4	203.2	Interchangeable 3-3/8" SAE or 1/4" NPT both Ports. 2 ea. Inlet & outlet	49 (22)
	AGD-50	15000	1034	100	7	15000	1034	5000	345	N/A	N/A	50 Pa+Pa	3.9	63.9	Interchangeable 3-3/8" SAE or 1/4" NPT both Ports. 2 ea. Inlet & outlet	39 (18)
	AGD-62	5000	345	200	14	9000	620	5000	345	9000	620	60 Pa+Pa	6.2	101.8	Interchangeable 3-3/8" SAE or 1/4" NPT both Ports. 2 ea. Inlet & outlet	49 (22)
	AGD-75	12000	827	250	17	12000	827	5000	345	15000	1034	75 Pa+Pa	2.4	39.3	Interchangeable 3-3/8" SAE or 1/4" NPT both Ports. 2 ea. Inlet & outlet	39 (18)
	AGD-102	15000	1034	100	7	15000	1034	5000	345	15000	1034	100 Pa+ Pa	3.9	63.9	Interchangeable 3-3/8" SAE or 1/4" NPT both Ports. 2 ea. Inlet & outlet	49 (22)
	AGD-152	25000	1724	250	17	25000	1724	N/A		15000	1034	150 Pa+Pa	2.4	39.3	Interchangeable 3-3/8" SAE or 1/4" NPT both Ports. 2 ea. Inlet & outlet	49 (22)
Two Stage Model AGT	AGT-4	1250	86	1/4 ATM	1/4 ATM	1250	86	1250	86	N/A		4 Pa+Pa	10	164	3/8" NPT Both Ports	25 (11)
	AGT-7/15	6 Pa to 2500 ¹	0 Pa to 172 ¹	25	1.7	5000	345	5000	345	4000	270	15 Pa+2 Ps	13.2	210.3	Inlet Port 3/8" NPT Outlet Port: 3/8" SAE or 1/4" NPT (Both Ports)	40 (18)
	AGT-7/30	3 Pa to 1500 ¹	0 Pa to 102 ¹	25	1.7	9000	620	5000	345	9000	620	30 Pa+4 Ps	13.2	210.3	Inlet Port 3/8" NPT Outlet Port: 3/8" SAE or 1/4" NPT (Both Ports)	41 (19)
	AGT-14/32	12 Pa to 2500 ¹	12 Pa to 172 ¹	25	1.7	5000	345	5000	345	4000	270	30 Pa+2 Ps	13.2	210.3	Inlet Port: 3/8" NPT Outlet Port: 3/8" SAE or 1/4" NPT (Both Ports)	48 (21)
	AGT-14/62	4 Pa to 2500 ¹	4 Pa to 102 ¹	25	1.7	9000	620	5000	345	9000	620	60 Pa+4 Ps	13.2	210.3	Inlet Port: 3/8" NPT Outlet Port: 3/8" SAE or 1/4" NPT (Both Ports)	41 (19)
	AGT-15/30	15 Pa to 1500 ¹	15 Pa to 102 ¹	50	3.5	9000	620	5000	345	9000	620	30 Pa+2 Ps	6.2	101.8	Interchangeable 3/8" SAE or 1/4" NPT (Both Ports) Both Ports	39 (18)
	AGT-15/50	15 Pa to 1500 ¹	15 Pa to 102 ¹	100	7	15000	1034	5000	345	15000	1034	50 Pa+3.3 Ps	6.2	102	Interchangeable 3-3/8" SAE or 1/4" NPT (Both Ports) Both Ports	38 (17)